^{57}FE MÖSSBAUER DATA

Simulation details for [LFe$_3$(PhPz)$_3$FFe][OTf] (1): The Mössbauer spectrum of **1** features an intense signal around 3 mm/s characteristic of a high-spin Fe(II) center. Fitting a quadrupole doublet for this peak led to a model that accounted for ~75% of the overall signal, with a second doublet satisfactorily accounting for the rest of the signal (Figure 1). The final refinement spli t the 75%-abundant high-spin Fe(II) signal into three equally populated doublets (Figure 2).

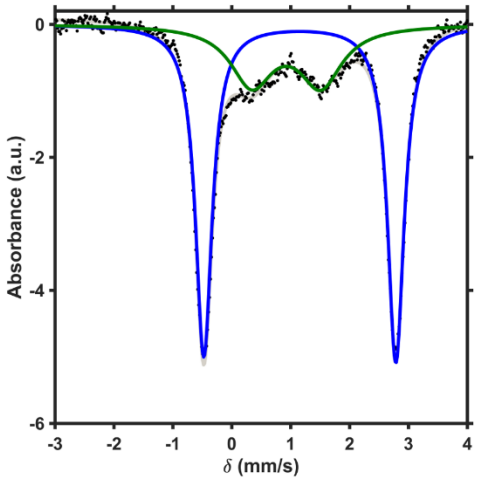

Figure 1. Mössbauer spectrum of **1** (black dots) fit with two doublets in ~3:1 ratio refined with parameters: δ = 1.156 mm/s; ΔE_q = 3.260 mm/s (blue trace) and δ = 0.925 mm/s; ΔE_q = 1.171 mm/s (green trace). The overall fit is the gray trace.

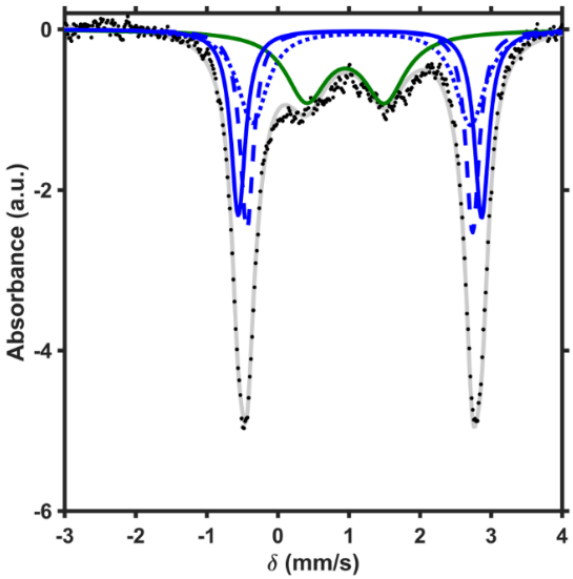

	δ (mm/s)	$\lvert\Delta E_q\rvert$ (mm/s)	Γ	Rel. %
———	1.156	3.424	0.25	25
– – –	1.152	3.176	0.23	25
·····	1.178	3.065	0.50	25
———	0.951	1.099	0.70	25

Figure 2. Zero applied field ^{57}Fe Mössbauer spectrum of [LFe$_3$F(PhPz)$_3$Fe][OTf] (**1**). The data (black dots) was fit to four Fe quadrupole doublets (gray trace). The blue traces represent signals assigned to the high-spin Fe^{II} of the tri-iron core and the green trace is assigned to the apical high-spin Fe^{II}.

Simulation details for [LFe$_3$(PhPz)$_3$FFe][OTf]$_2$ (2): The Mössbauer spectrum of **2** was fit by first fitting the signal at 3 mm/s to high-spin Fe(II) (Figure 3A); this fit accounted for ~50% the total spectrum. The remaining spectrum was fit with two nearly equal doublets (Figure 3B); other combinations of this signal to arrive at alternative parameters for these two signals could not be satisfactorily modeled, so these are not included. The final fit split the 50%-abundant Fe(II) signal into two equal doublets (Figure 4).

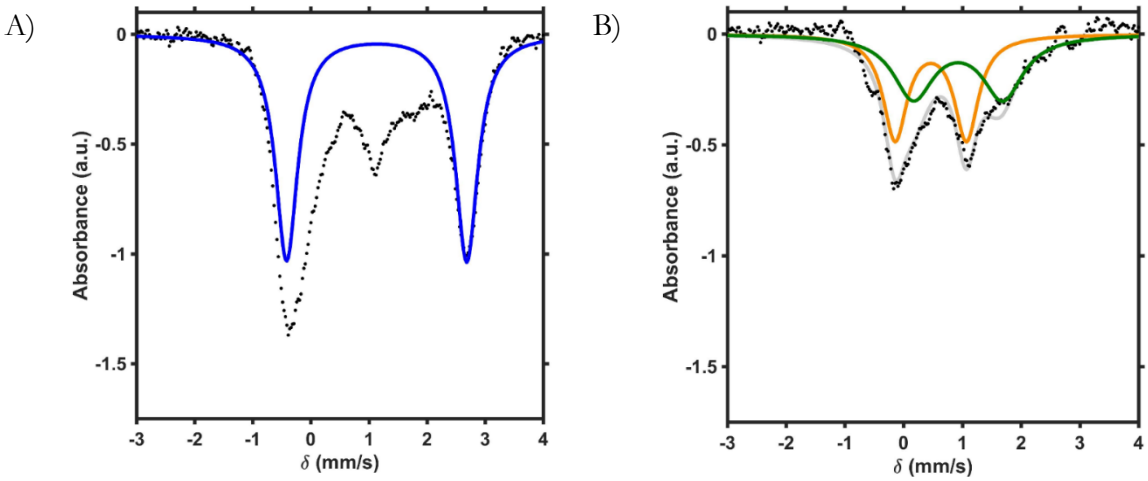

Figure 3. Mössbauer spectrum of **2** (black dots) (A) fit with a single doublet refined with parameters consistent with high-spin Fe(II): δ = 1.132 mm/s; ΔE_q = 3.101 mm/s (blue trace). (B) Mössbauer spectrum of **2** with this Fe(II) doublet subtracted (black dots) and two equally abundant signals fit (gray trace): δ = 0.462 mm/s; ΔE_q = 1.213 mm/s (orange trace), and δ = 0.928 mm/s; ΔE_q = 1.522 mm/s (green trace).

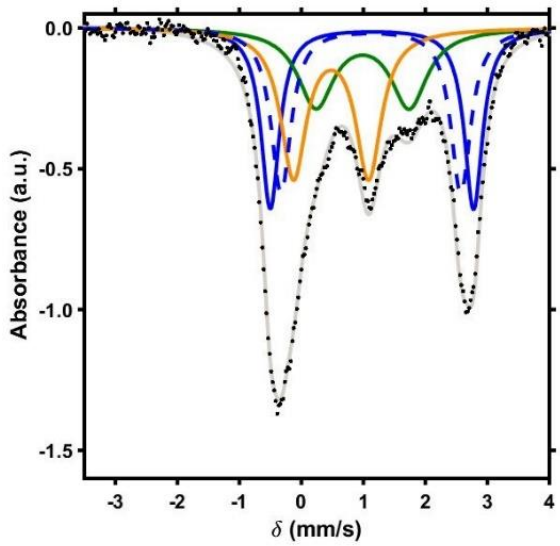

	δ (mm/s)	$\lvert\Delta E_q\rvert$ (mm/s)	Γ	Rel. %
	1.138	3.297	0.35	25
	1.122	2.899	0.39	25
	0.479	1.211	0.50	29
	0.987	1.504	0.70	21

Figure 4. Zero applied field ^{57}Fe Mössbauer spectrum of [LFe$_3$F(PhPz)$_3$Fe][OTf]$_2$ (**2**). The data (black dots) was fit to four Fe quadrupole doublets (gray trace). The blue traces represent signals assigned to the high-spin Fe^{II} of the tri-iron core, the orange trace is assigned to high-

spin Fe^{III} in the tri-iron core, and the green trace is assigned to the apical high-spin Fe^{II}. The best fit was obtained by having a slight deviation from four equally abundant Fe centers.

Simulation details for $[LFe_3(PhPz)_3FFe(CH_3CN)][OTf]_3$ (3): The Mössbauer spectrum of **3** contains three easily observable features, which was first approximated by fitting two doublets (Figure 5A). This fit shows inadequate modeling for the signal around 2 mm/s, so a third doubled was modeled in (Figure 5B-D). This fit led to three signals in an approximately 1:1:2 ratios. Of the possible distribution of these three signals, the fit in Figure 5D is favored, because it has isomer shifts self-consistent for the two Fe(III) centers (0.4 – 0.5 mm/s) and the Fe(II) center (1.00 – 1.15 mm/s) of the 'tri-iron' core of our related iron clusters presented here and previously reported. Furthermore, the third signal is most consistent with a high-spin five-coordinate Fe(II) (~0.1 mm/s lower than the corresponding six-coordinate Fe(II) signal), which is in agreement of the coordination of the apical Fe(II) in the crystal structure of **3**. The final fit was refined by splitting the 50%-abundant Fe(III) signal into two equal signals (Figure 6).

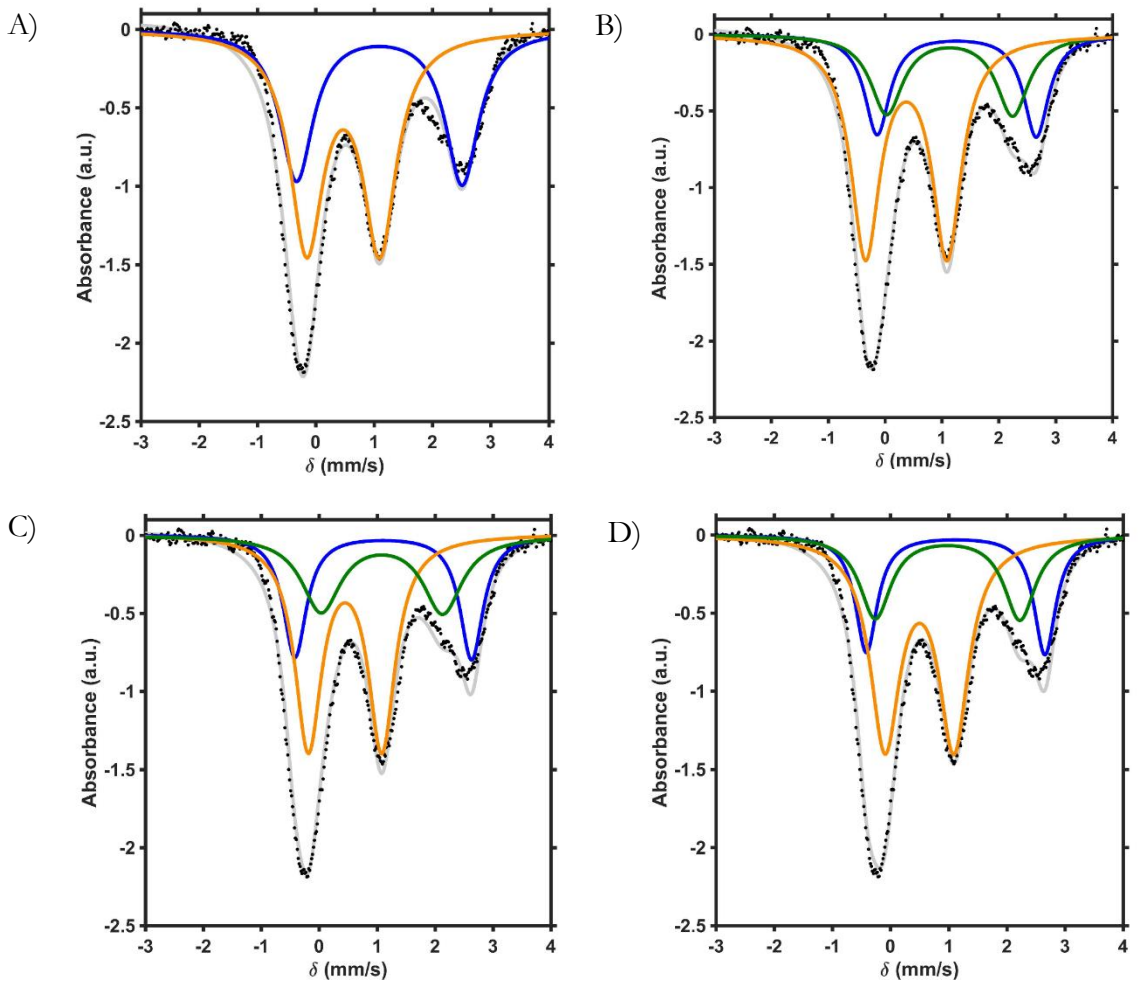

Figure 5. Mössbauer spectrum of **3** (black dots) (A) fit with two signals (gray trace) refined with parameters: δ = 1.091 mm/s; ΔE_q = 2.841 mm/s (blue trace), and δ = 0.471 mm/s; ΔE_q = 1.253 mm/s (orange trace). (B) Mössbauer spectrum of **3** fit with three signals in a 1:1:2

ratio (gray trace) with the parameters: δ = 1.261 mm/s; ΔE_q = 2.797 mm/s (blue trace), δ = 1.137 mm/s; ΔE_q = 2.216 mm/s (green trace), and δ = 0.374 mm/s; ΔE_q = 1.433 mm/s (orange trace). (C) Mössbauer spectrum of **3** fit with three signals in a 1:1:2 ratio (gray trace) with the parameters: δ = 1.106 mm/s; ΔE_q = 3.050mm/s (blue trace), δ = 1.083 mm/s; ΔE_q = 2.098 mm/s (green trace), and δ = 0.447 mm/s; ΔE_q = 1.269 mm/s (orange trace). (D) Mössbauer spectrum of **3** fit with three signals in a 1:1:2 ratio (gray trace) with the parameters: δ = 1.120 mm/s; ΔE_q = 3.071 mm/s (blue trace), δ = 0.981 mm/s; ΔE_q = 2.486 mm/s (green trace), and δ = 0.498 mm/s; ΔE_q = 1.186 mm/s (orange trace).

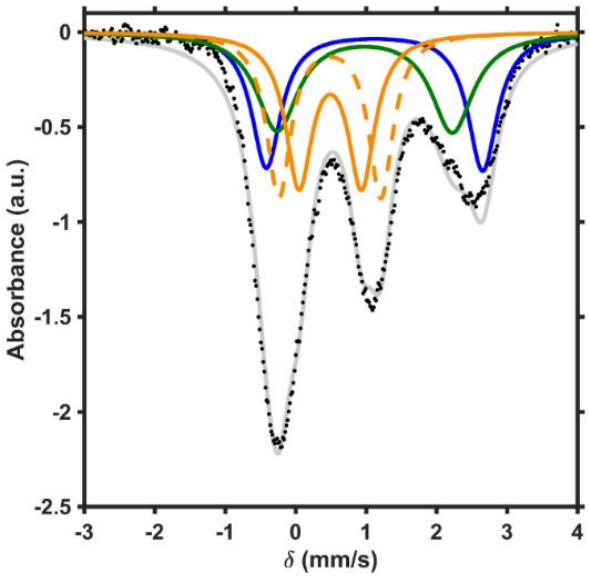

	δ (mm/s)	$\lvert\Delta E_q\rvert$ (mm/s)	Γ	Rel. %
	1.120	3.071	0.51	25
	0.492	0.889	0.46	25
	0.487	1.449	0.42	25
	0.981	2.486	0.72	25

Figure 6. Zero applied field ^{57}Fe Mössbauer spectrum of $[LFe_3F(PhPz)_3Fe(CH_3CN)][OTf]_3$ (**3**). The data (black dots) was fit to four Fe quadrupole doublets (gray trace). The blue trace represents the signal assigned to the high-spin Fe^{II} of the tri-iron core, the orange traces are assigned to high-spin Fe^{III} in the tri-iron core, and the green trace is assigned to the apical high-spin Fe^{II}.

Simulation details for $LFe_3(PhPz)_3FFe(NO)$ (5-NO): The Mössbauer spectrum of **5-NO** displays three readily distinguished signals. The major two were initially fit with a single doublet, which had parameters consistent with high-spin Fe(II) (Figure 7); the remaining signal was fit in a 3:1 ratio relative to the first signal. The final fit split the high-spin Fe(II) doublet into three equal doublets (Figure 8).

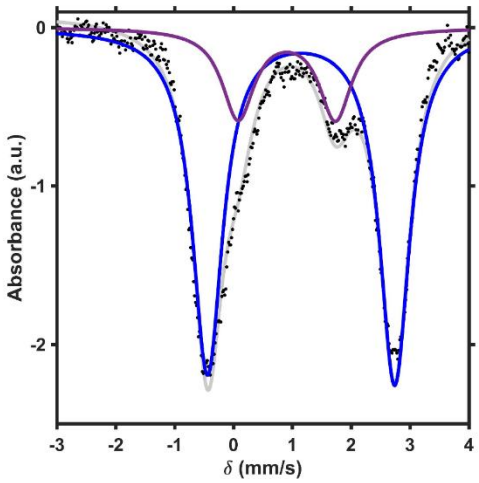

Figure 7. Mössbauer spectrum of **5-NO** (black dots) fit with two doublets in a ~3:1 ratio (gray trace) with the parameters: δ = 1.149 mm/s; ΔE_q = 3.177 mm/s (blue trace), and δ = 0.906 mm/s; ΔE_q = 1.651 mm/s (purple trace).

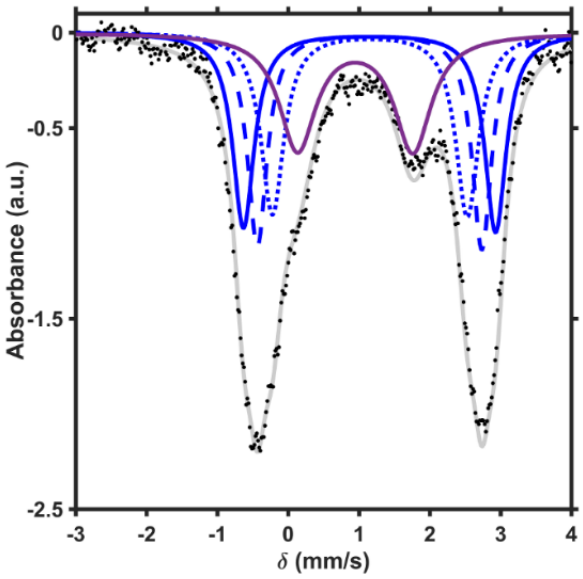

	δ (mm/s)	$\lvert\Delta E_q\rvert$ (mm/s)	Γ	Rel. %
———	1.148	3.561	0.37	25
– – –	1.150	3.172	0.33	25
·····	1.153	2.753	0.39	25
———	0.947	1.629	0.63	25

Figure 8. Zero applied field ^{57}Fe Mössbauer spectrum of $LFe_3F(PhPz)_3Fe(NO)$ (**5-NO**). The data (black dots) was fit to four Fe quadrupole doublets (gray trace). The blue traces represent the signal assigned to the high-spin Fe^{II} of the tri-iron core and the purple trace is assigned to the apical $\{FeNO\}^8$.

Simulation details for [LFe$_3$(PhPz)$_3$FFe(NO)][OTf] (1-NO): The Mössbauer spectrum of **1-NO** contains four distinguishable signals (one being a shoulder on the peak below 0 mm/s). These four signals were fit to two doublets based on their relative intensities and had an approximate 3:1 ratio (Figure 9). The final fit refined the intense Fe(II) doublet into three equal signals (Figure 10).

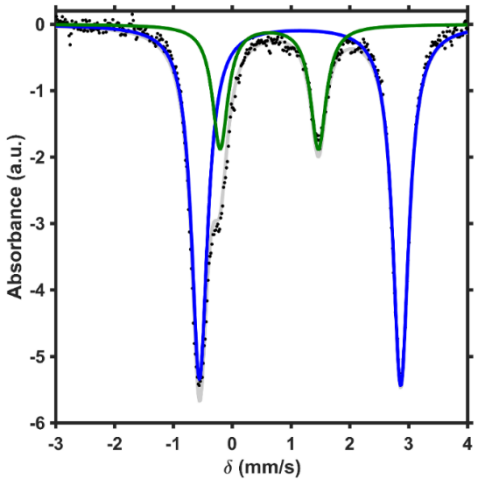

Figure 9. Mössbauer spectrum of **1-NO** (black dots) fit with two doublets in a ~3:1 ratio (gray trace) with the parameters: δ = 1.139 mm/s; ΔE_q = 3.308 mm/s (blue trace), and δ = 0.609 mm/s; ΔE_q = 1.631 mm/s (green trace).

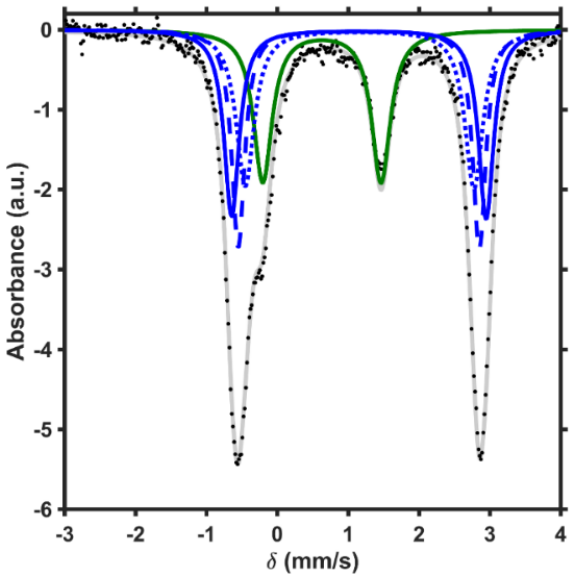

	δ (mm/s)	$\lvert\Delta E_q\rvert$ (mm/s)	Γ	Rel. %
———	1.152	3.592	0.26	25
– – –	1.150	3.403	0.22	25
·····	1.162	3.229	0.31	25
———	0.630	1.669	0.32	25

Figure 10. Zero applied field ^{57}Fe Mössbauer spectrum of [LFe$_3$F(PhPz)$_3$Fe(NO)][OTf] (**1-NO**). The data (black dots) was fit to four Fe quadrupole doublets (gray trace). The blue traces represent the signal assigned to the high-spin Fe^{II} of the tri-iron core and the green trace is assigned to the apical {FeNO}^{7}.

Simulation details for [LFe$_3$(PhPz)$_3$FFe(NO)][OTf]$_2$ (2-NO): The Mössbauer spectrum of **2-NO** displays four readily-distinguished signals. The signal above 3 mm/s was initially fit as high-spin Fe(II), and this doublet accounts for 50% of the overall spectrum (Figure 11A). The remaining signal was fit as two equally abundant doublets in three different ways (Figures 11B-D). The fit in Figure S39B gives unreasonable isomer shifts of -0.1 and 0.2 mm/s (orange and green traces, respectively). The fits in Figures 11C and 11D are only slightly different, but the fit in Figure 11D gives parameters that are more self-consistent with isomer shift values for the Fe(III) center of the 'tri-iron core' (0.4 mm/s; orange trace) and the {FeNO}^{7} center of the fluoride-bridged tetranuclear iron clusters (0.6 mm/s; green trace; see parameter refinement for **1-NO**). The final fit split the 50%-abundant Fe(II) signal into two doublets (Figure 12).

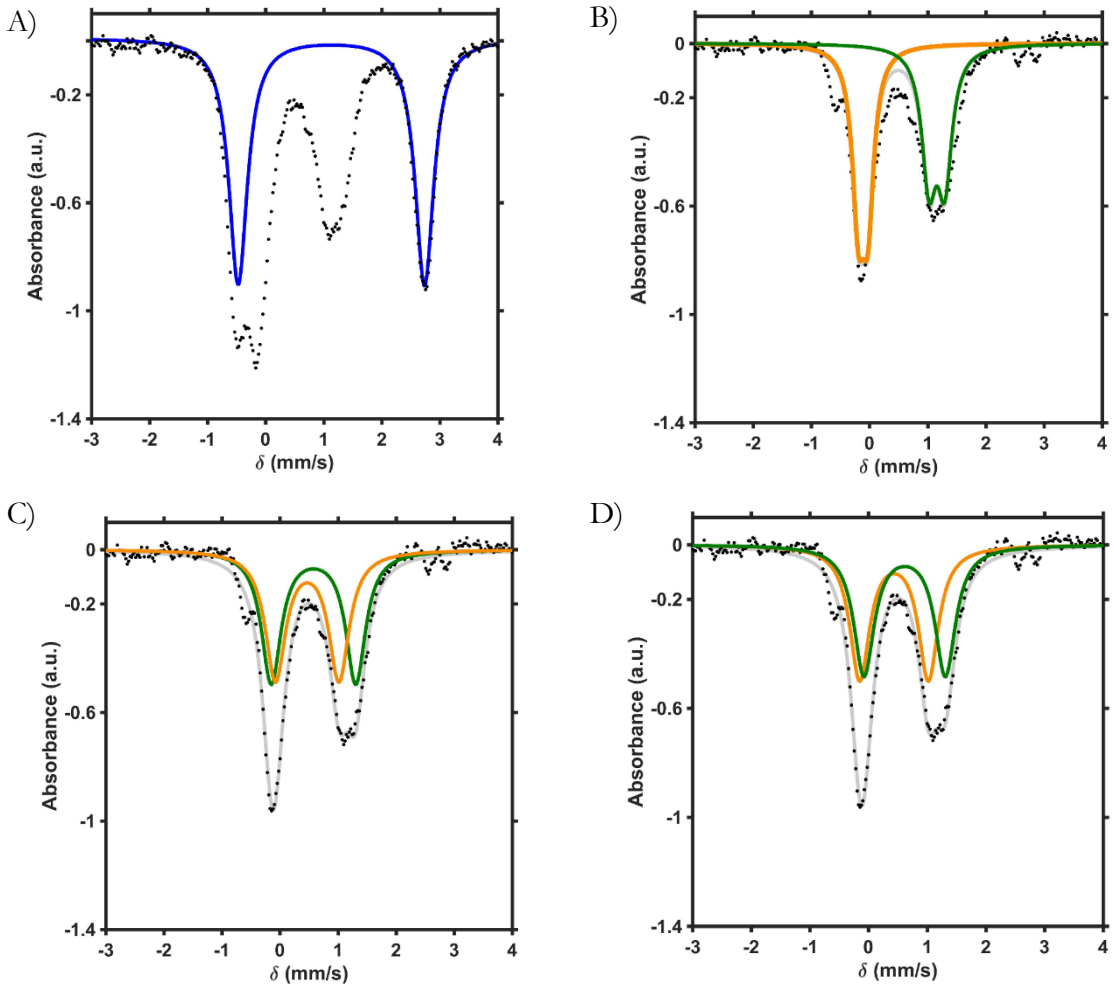

Figure 11. Mössbauer spectrum of **2-NO** (black dots) (A) fit with a single doublet refined with parameters consistent with high-spin Fe(II): δ = 1.132 mm/s; ΔE_q = 3.211 mm/s (blue trace). (B) Mössbauer spectrum of **2-NO** with this Fe(II) doublet subtracted (black dots) and two equally abundant signals fit (gray trace): δ = -0.111 mm/s; ΔE_q = 0.165 mm/s (orange trace), and δ = 1.158 mm/s; ΔE_q = 0.270 mm/s (green trace). (C) Mössbauer spectrum of **2-NO** with this Fe(II) doublet subtracted (black dots) and two equally abundant signals fit (gray trace): δ = 0.577 mm/s; ΔE_q = 1.456 mm/s (green trace), and δ = 0.469 mm/s; ΔE_q = 1.094

mm/s (orange trace). (D) Mössbauer spectrum of **2-NO** with this Fe(II) doublet subtracted (black dots) and two equally abundant signals fit (gray trace): δ = 0.616 mm/s; ΔE_q = 1.387 mm/s (green trace), and δ = 0.435 mm/s; ΔE_q = 1.171 mm/s (orange trace).

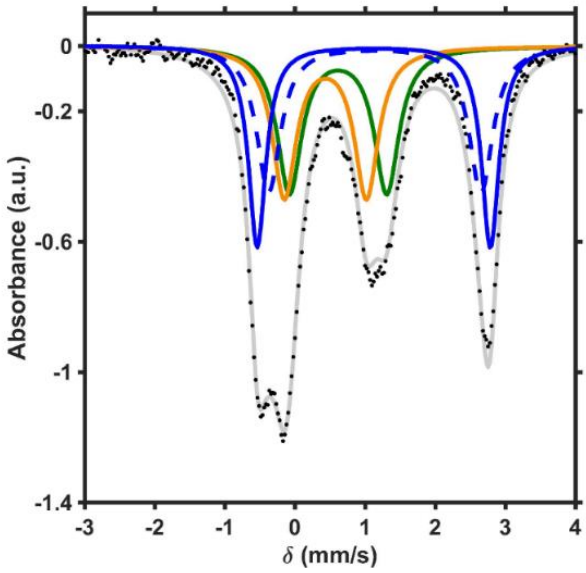

	δ (mm/s)	$\lvert\Delta E_q\rvert$ (mm/s)	Γ	Rel. %
———	1.121	3.309	0.30	25
– – –	1.150	3.026	0.46	25
———	0.435	1.171	0.41	25
———	0.616	1.387	0.42	25

Figure 12. Zero applied field ^{57}Fe Mössbauer spectrum of $[LFe_3F(PhPz)_3Fe(NO)][OTf]_2$ (**2-NO**). The data (black dots) was fit to four Fe quadrupole doublets (gray trace). The blue traces represent the signal assigned to the high-spin Fe^{II} of the tri-iron core, the orange trace is assigned to the high-spin Fe^{III} in the tri-iron core, and the green trace is assigned to the apical $\{FeNO\}^7$.

Simulation details for $[LFe_3(PhPz)_3FFe(NO)][OTf]_3$ (3-NO): The Mössbauer spectrum of **3-NO** displays three major features (instead of the expected eight for four Fe centers). The peak around 3 mm/s was modeled as a high-spin Fe(II) with parameters consistent with other Fe(II) centers in the 'tri-iron core' of the tetranuclear clusters; this fit accounted for 25% of the total signal (Figure 13A). Subtracting this doublet from the data, the remaining signal could be fit reasonably well with either one or two equally abundant quadrupole doublets (Figures 13B and 13C), however these fits were ruled out since they were inconsistent with our crystallographic analysis of **3-NO**. There are many possible ways to fit 3 doublets in this residual signal; below are shown three fits that give reasonable fit parameters for two high-spin Fe(III) centers and a high-spin five-coordinate $\{FeNO\}^7$ (Figure 13D-F). The fit in Figure 13F gave parameters the most self-consistent within this series of clusters, and was used for the final refinement (Figure 14).

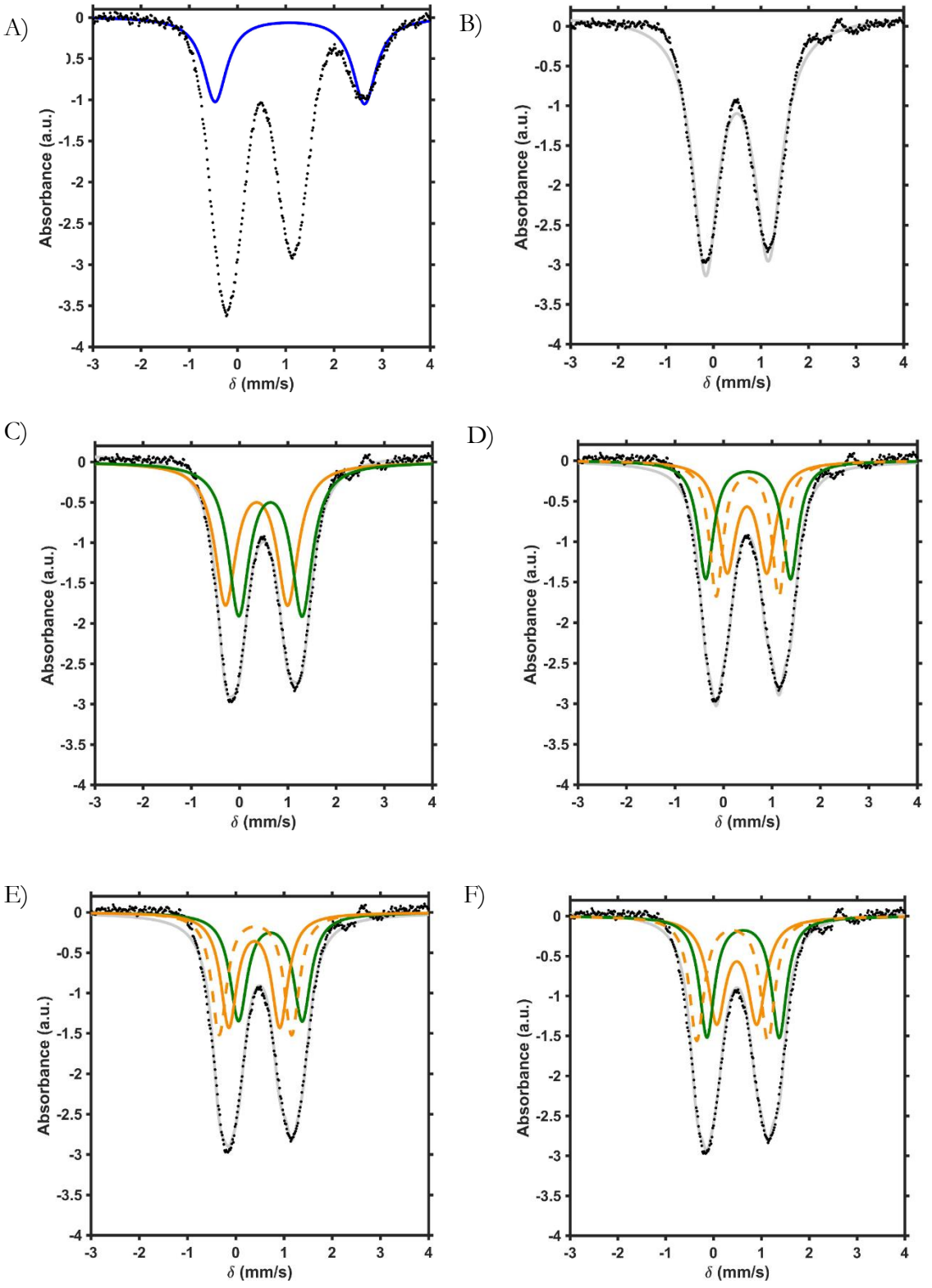

Figure 13. Mössbauer spectrum of **3-NO** (black dots) (A) fit with a single doublet refined with parameters consistent with high-spin Fe(II): δ = 1.087 mm/s; ΔE_q = 3.100 mm/s (blue trace). (B) Mössbauer spectrum of **3-NO** with this Fe(II) doublet subtracted (black dots) and

fit with a single quadrupole doublet (gray trace): δ = 0.501 mm/s; ΔE_q = 1.319 mm/s. (C) Mössbauer spectrum of **3-NO** with this Fe(II) doublet subtracted (black dots) and two equally abundant signals fit (gray trace): δ = 0.354 mm/s; ΔE_q = 1.291 mm/s (orange trace), and δ = 0.643 mm/s; ΔE_q = 1.314 mm/s (green trace). (D) Mössbauer spectrum of **3-NO** with this Fe(II) doublet subtracted (black dots) and three equally abundant signals fit (gray trace): δ = 0.488 mm/s; ΔE_q = 0.819 mm/s (solid orange trace), and δ = 0.499 mm/s; ΔE_q = 1.292 mm/s (dashed orange trace), and δ = 0.512 mm/s; ΔE_q = 1.750 mm/s (green trace). (E) Mössbauer spectrum of **3-NO** with this Fe(II) doublet subtracted (black dots) and three equally abundant signals fit (gray trace): δ = 0.387 mm/s; ΔE_q = 1.058 mm/s (solid orange trace), and δ = 0.409 mm/s; ΔE_q = 1.503 mm/s (dashed orange trace), and δ = 0.719 mm/s; ΔE_q = 1.321 mm/s (green trace). (F) Mössbauer spectrum of **3-NO** with this Fe(II) doublet subtracted (black dots) and three equally abundant signals fit (gray trace): δ = 0.486 mm/s; ΔE_q = 0.840 mm/s (solid orange trace), and δ = 0.395 mm/s; ΔE_q = 1.486 mm/s (dashed orange trace), and δ = 0.620 mm/s; ΔE_q = 1.512 mm/s (green trace).

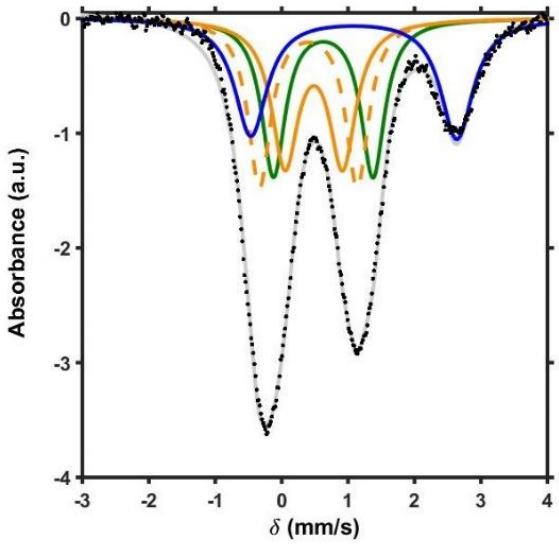

	δ (mm/s)	$\lvert\Delta E_q\rvert$ (mm/s)	Γ	Rel. %
	1.087	3.100	0.59	25
	0.484	0.868	0.49	25
	0.402	1.471	0.41	25
	0.615	1.507	0.44	25

Figure 14. Zero applied field ^{57}Fe Mössbauer spectrum of $[LFe_3F(PhPz)_3Fe(NO)][OTf]_3$ (**3-NO**). The data (black dots) was fit to four Fe quadrupole doublets (gray trace). The blue trace represents the signal assigned to the high-spin Fe^{II} of the tri-iron core, the orange traces are assigned to the high-spin Fe^{III} in the tri-iron core, and the green trace is assigned to the apical $\{FeNO\}^7$.

Simulation details for $[LFe_3(PhPz)_3FFe(NO)][OTf]_3[SbCl_6]$ (4-NO): The Mössbauer spectrum of **4-NO** displays two broad features, which were adequately fit as a single quadrupole doublet (Figure 15). Since it is likely that the Fe(III) signals are overlapping with the $\{FeNO\}^7$ signal (see Mössbauer spectra of **2-NO** and **3-NO**), modeling the four separate Fe centers is not included. This spectrum is consistent, however, with our assignment of **4-NO** as a cluster containing no Fe(II) centers, since there the characteristic signal around 3 mm/s is absent.

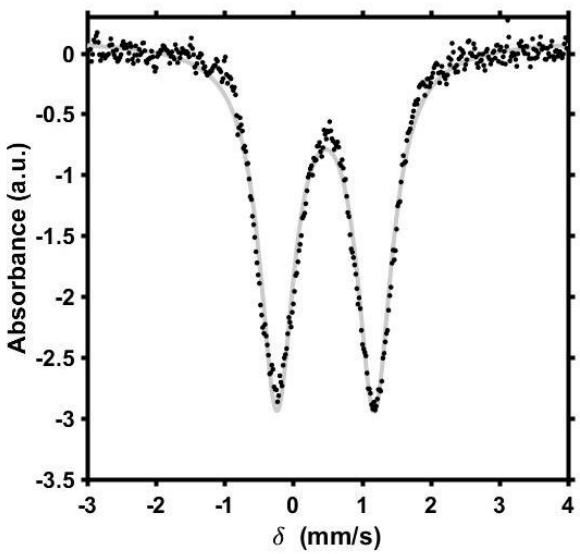

	δ (mm/s)	$\lvert\Delta E_q\rvert$ (mm/s)	Γ	Rel. %
	0.471	1.420	0.61	100

Figure 15. Zero applied field ^{57}Fe Mössbauer spectrum of $[LFe_3F(PhPz)_3Fe(NO)][OTf]_3[SbCl_6]$ (**4-NO**). The data (black dots) was fit to a single Fe quadrupole doublet (gray trace). We postulate that the signal for the apical $\{FeNO\}^7$ is overlapping with the doublet(s) for the high-spin Fe(III) in the 'tri-iron core'.

Simulation details for 1-[OTf]: The spectrum displays three discernable peaks corresponding to two quadrupole doublets in ~ 1:2 ratio (Figure 16). The parameters of the more intense peak are consistent with a high-spin Fe(II) assignment, while the smaller doublet displays parameters consistent with high-spin Fe(III). The final fit split the large doublet into two equal signals (Figure 17).

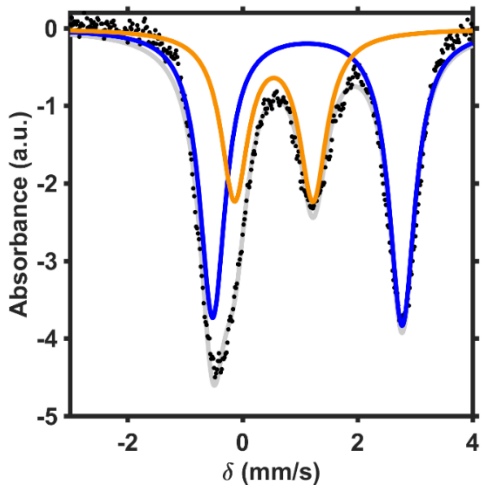

Figure 16. Mössbauer spectrum of **1-[OTf]** (black dots) fit with two doublets in a ~1:2 ratio (gray trace) with parameters $\delta = 0.543$ mm/s; $\Delta E_q = 1.366$ mm/s (orange trace) and $\delta = 1.126$ mm/s; $\Delta E_q = 3.294$ mm/s (blue trace).

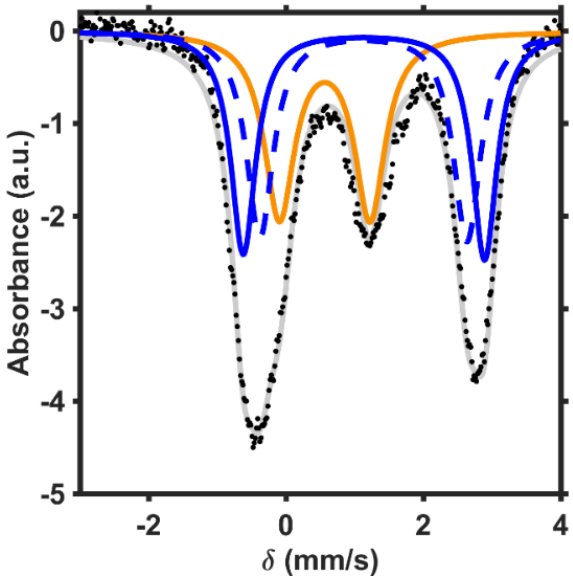

	δ (mm/s)	$\lvert\Delta E_q\rvert$ (mm/s)	Rel. %
———	1.135	3.513	33
– – –	1.127	3.016	33
———	0.563	1.318	33

Figure 17. Zero applied field Mössbauer spectrum of **1-[OTf]** (black dots) fit with three quadrupole doublets. The blue traces are assigned to high-spin Fe(II) and the orange trace is assigned as high-spin Fe(III).

Simulation details for 2-[OTf]: The spectrum displays four discernable peaks corresponding to two quadrupole doublets in ~ 1:2 ratio (Figure 18). The parameters of the more intense peak are consistent with a high-spin Fe(III) assignment, while the smaller doublet displays parameters consistent with high-spin Fe(II). The final fit split the large doublet into two equal signals (Figure 19).

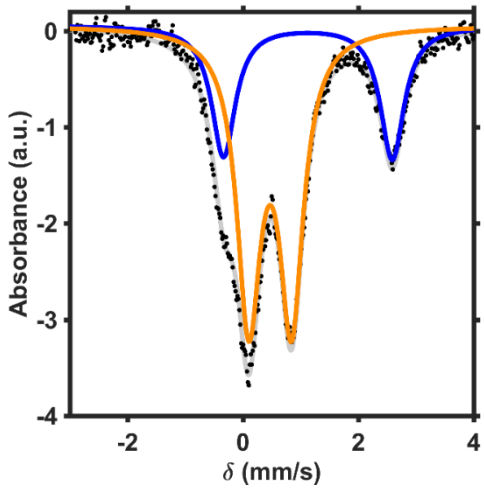

Figure 18. Mössbauer spectrum of **2-[OTf]** (black dots) fit with two doublets in a ~1:2 ratio (gray trace) with parameters $\delta = 0.469$ mm/s; $\Delta E_q = 0.740$ mm/s (orange trace) and $\delta = 1.124$ mm/s; $\Delta E_q = 2.926$ mm/s (blue trace).

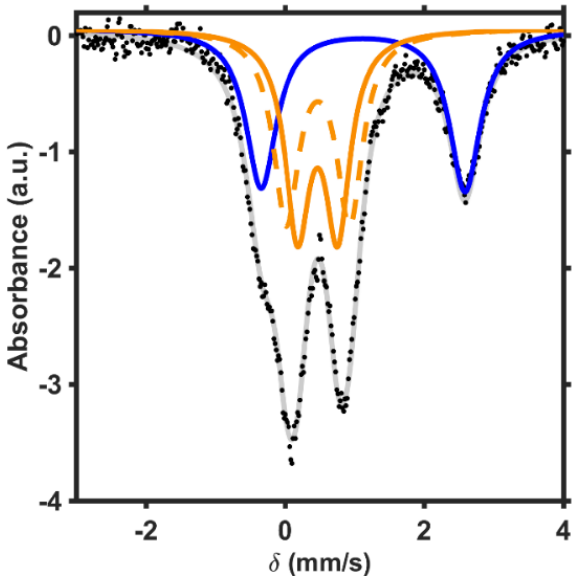

	δ (mm/s)	$\lvert\Delta E_q\rvert$ (mm/s)	Rel. %
———	1.119	2.931	33
———	0.468	0.578	33
- - -	0.423	0.913	33

Figure 19. Zero applied field Mössbauer spectrum of **2-[OTf]** (black dots) fit with three quadrupole doublets. The blue trace is assigned to high-spin Fe(II) and the orange traces are assigned to high-spin Fe(III).

Simulation details for 3-[OTf]: The spectrum displays a single quadrupole doublet signal. Although three Fe(III) signals are expected, the best fit was obtained with only one set of parameters (Figure 20).

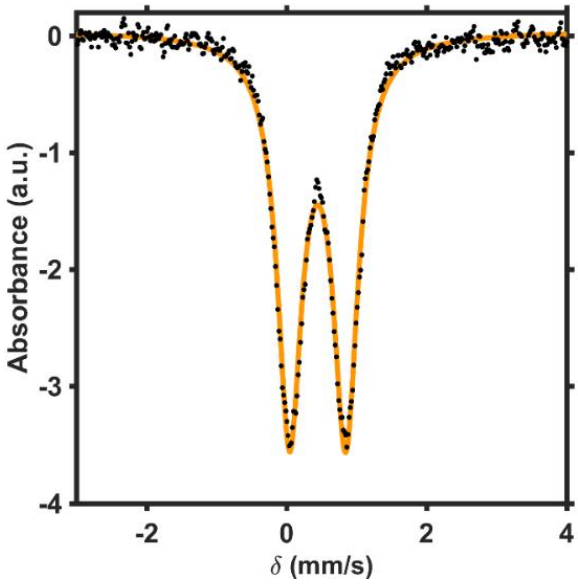

	δ (mm/s)	$\lvert\Delta E_q\rvert$ (mm/s)	Rel. %
	0.443	0.804	100

Figure 20. Zero applied field Mössbauer spectrum of **3-[OTf]** (black dots) fit to a single quadrupole doublet (orange trace); this signal is assigned to the high-spin Fe(III) centers in the cluster.

Simulation details for 1-[BAr$^F_4$]: The spectrum displays three discernable peaks corresponding to two quadrupole doublets in ~ 1:2 ratio (Figure 21). The parameters of the more intense peak are consistent with a high-spin Fe(II) assignment, while the smaller doublet displays parameters consistent with high-spin Fe(III). The final fit split the large doublet into two equal signals (Figure 22).

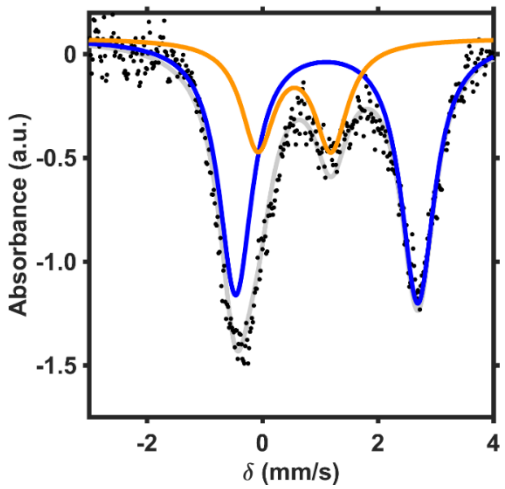

Figure 21. Mössbauer spectrum of **1-[BAr$^F_4$]** (black dots) fit with two doublets in a ~1:2 ratio (gray trace) with parameters δ = 0.556 mm/s; ΔE_q = 1.267 mm/s (orange trace) and δ = 1.115 mm/s; ΔE_q = 3.153 mm/s (blue trace).

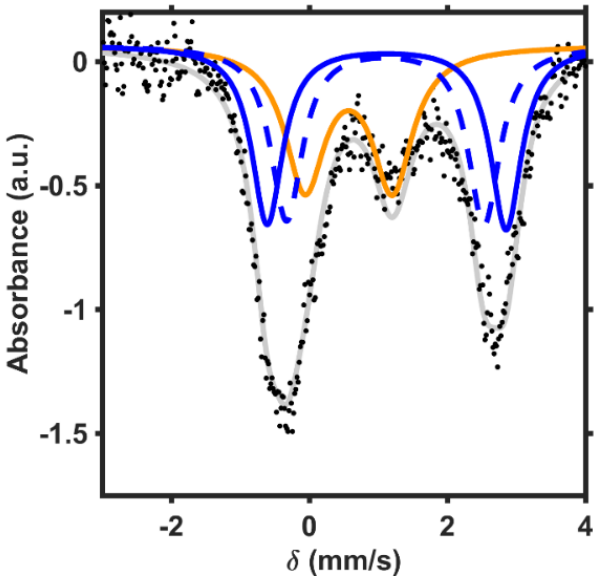

	δ (mm/s)	$\lvert\Delta E_q\rvert$ (mm/s)	Rel. %
———	1.119	3.460	33
– – –	1.099	2.860	33
———	0.570	1.266	33

Figure 22. Zero applied field Mössbauer spectrum of **1-[BAr$^{F}_{4}$]** (THF solution [250 mM H_2O]; black dots) fit with three quadrupole doublets. The blue traces are assigned to high-spin Fe(II) and the orange trace is assigned to high-spin Fe(III).

Simulation details for 2-[BAr$^{F}_{4}$]: The spectrum displays four discernable peaks corresponding to two quadrupole doublets in ~ 1:2 ratio (Figure 23). The parameters of the more intense peak are consistent with a high-spin Fe(III) assignment, while the smaller doublet displays parameters consistent with high-spin Fe(II). The final fit split the large doublet into two equal signals (Figure 24).

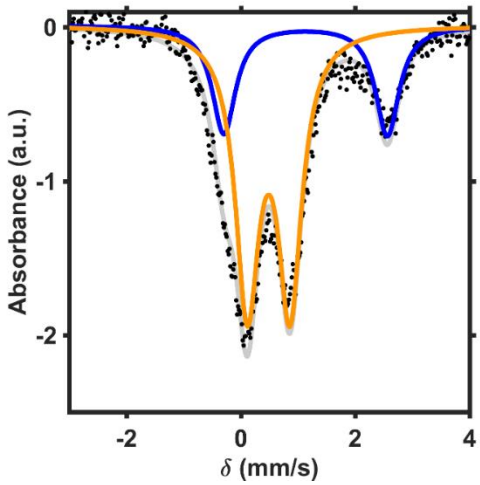

Figure 23. Mössbauer spectrum of **2-[BAr$^{F}_{4}$]** (black dots) fit with two doublets in a ~1:2 ratio (gray trace) with parameters δ = 0.485 mm/s; ΔE_q = 0.746 mm/s (orange trace) and δ = 1.132 mm/s; ΔE_q = 2.858 mm/s (blue trace).

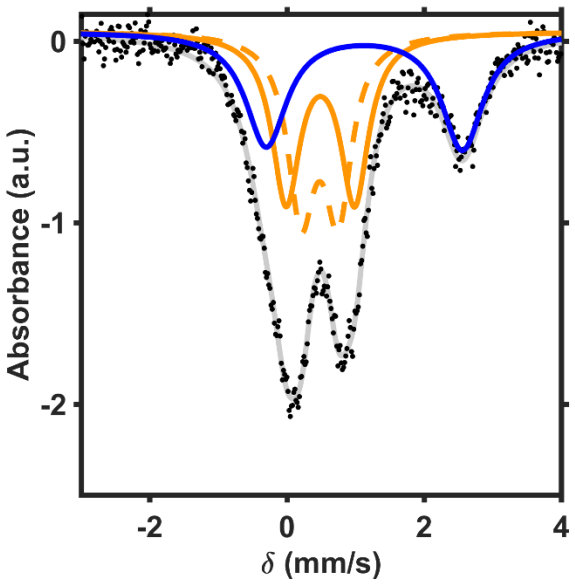

	δ (mm/s)	$\lvert\Delta E_q\rvert$ (mm/s)	Rel. %
———	1.128	2.858	33
———	0.487	0.999	33
- - -	0.478	0.540	33

Figure 24. Zero applied field Mössbauer spectrum of **2-[BAr$^{F}_{4}$]** (THF solution [250 mM H_2O]; black dots) fit with three quadrupole doublets. The blue trace is assigned to high-spin Fe(II) and the orange traces are assigned to high-spin Fe(III).

Simulation details for 3-[BAr$^{F}_{4}$]: The spectrum displays a single quadrupole doublet signal. Although three Fe(III) signals are expected, the best fit was obtained with only one set of parameters (Figure 25).

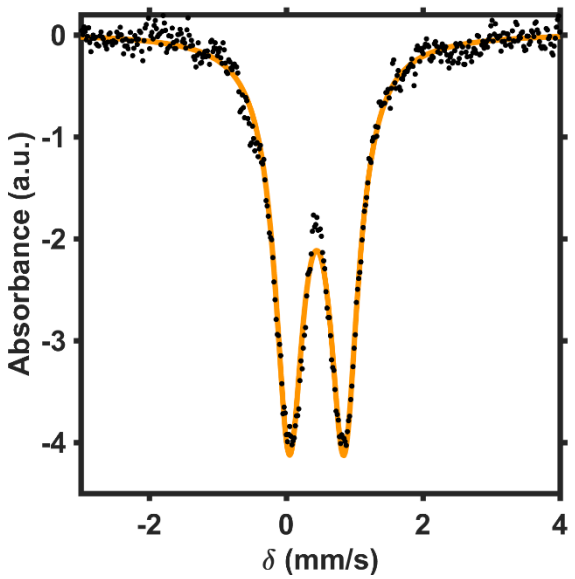

	δ (mm/s)	$\lvert\Delta E_q\rvert$ (mm/s)	Rel. %
———	0.444	0.800	100

Figure 25. Zero applied field Mössbauer spectrum of **3-[BAr$^{F}_{4}$]** (THF solution [250 mM H_2O]; black dots) fit with a single quadrupole doublet assigned to high-spin Fe(III) centers.

Simulation details for 5: The spectrum displays an apparently asymmetric quadrupole doublet signal. The data could be fit to a single quadrupole doublet (Figure 26). The final fit split this signal into three equally abundant Fe(II) centers, to account for the asymmetry of the doublet (Figure 27).

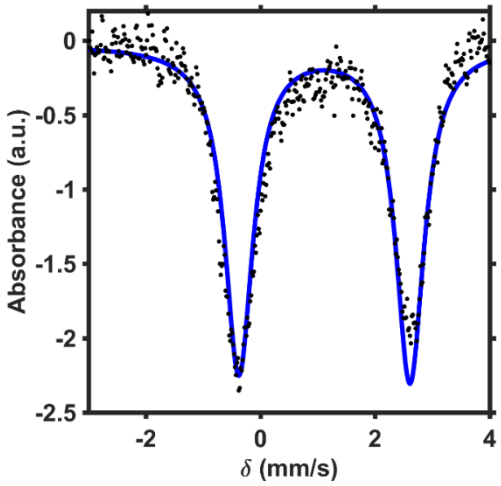

Figure 26. Mössbauer spectrum of **5** (black dots) fit with a single quadrupole doublet with parameters δ = 1.113 mm/s; ΔE_q = 2.985 mm/s (blue trace).

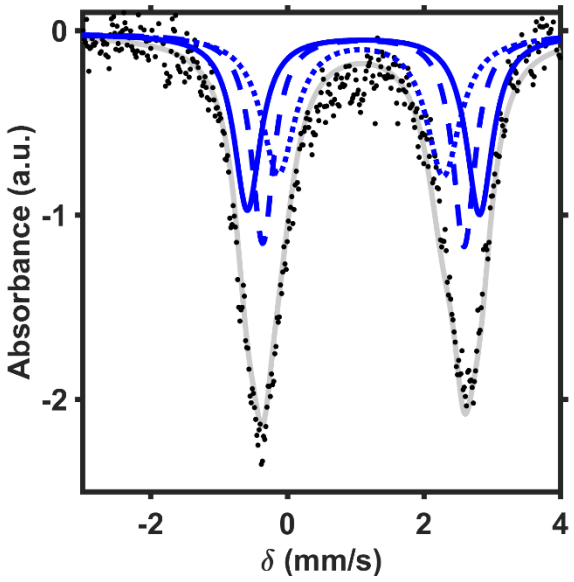

	δ (mm/s)	$\lvert\Delta E_q\rvert$ (mm/s)	Rel. %
———	1.115	3.399	33
– – –	1.115	2.947	33
·····	1.078	2.417	33

Figure 27. Zero applied field Mössbauer spectrum of **5** (black dots) fit with three quadrupole doublets. The blue traces are assigned to high-spin Fe(II).

Simulation details for 6-[BAr$^{F}_{4}$]: The spectrum displays four discernable peaks corresponding to two quadrupole doublets in ~ 1:2 ratio (Figure 28). The parameters of the more intense peak are consistent with a high-spin Fe(II) assignment, while the smaller doublet displays parameters consistent with high-spin Fe(III). The final fit split the large doublet into two equal signals (Figure 29).

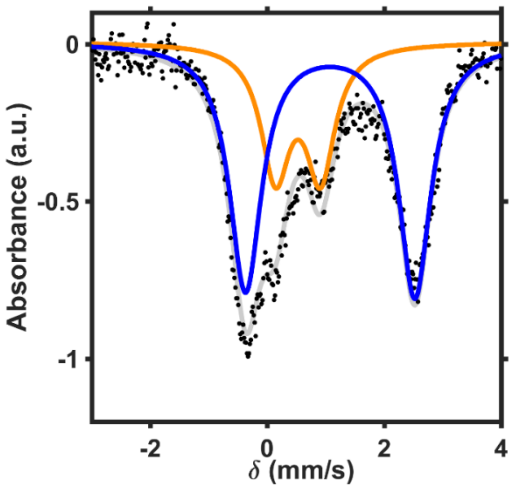

Figure 28. Mössbauer spectrum of **6-[BAr$^{F}_{4}$]** (black dots) fit with two doublets in a ~1:2 ratio (gray trace) with parameters δ = 0.525 mm/s; ΔE_q = 0.769 mm/s (orange trace) and δ = 1.075 mm/s; ΔE_q = 2.893 mm/s (blue trace).

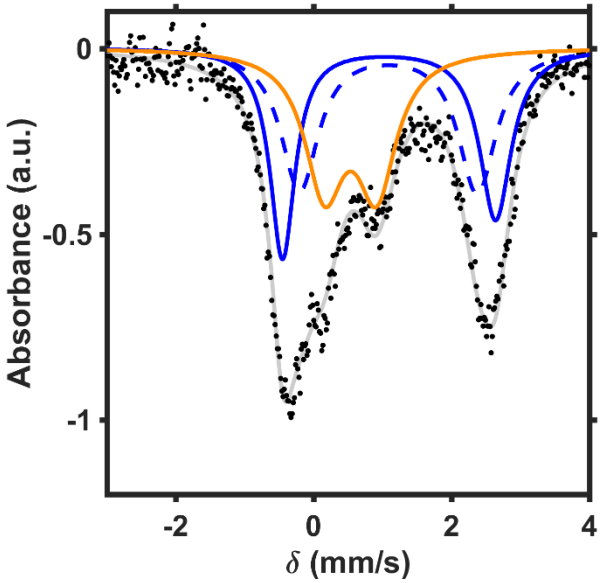

	δ (mm/s)	$\lvert\Delta E_q\rvert$ (mm/s)	Rel. %
———	1.093	3.091	33
– – –	1.083	2.576	33
———	0.534	0.756	33

Figure 29. Zero applied field Mössbauer spectrum of **6-[BAr$^{F}_{4}$]** (THF solution [250 mM H_2O]; black dots) fit with three quadrupole doublets. The blue traces are assigned to high-spin Fe(II) and the orange trace is assigned to high-spin Fe(III).

Simulation details for 7-[BAr$^{F}_{4}$]: The spectrum displays three discernable peaks, with a shoulder on the lowest peak, corresponding to two quadrupole doublets in ~ 1:2 ratio (Figure 30). The parameters of the more intense peak are consistent with a high-spin Fe(III) assignment, while the smaller doublet displays parameters consistent with high-spin Fe(III). The final fit split the large doublet into two equal signals (Figure 31).

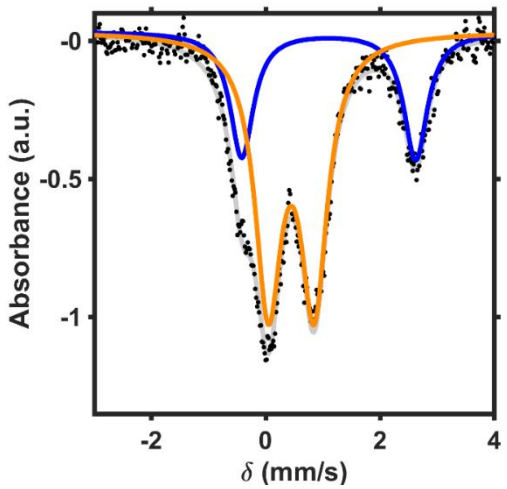

Figure 30. Mössbauer spectrum of **7-[BAr$^{F}_{4}$]** (black dots) fit with two doublets in a ~1:2 ratio (gray trace) with parameters δ = 0.447 mm/s; ΔE_q = 0.790 mm/s (orange trace) and δ = 1.109 mm/s; ΔE_q = 3.018 mm/s (blue trace).

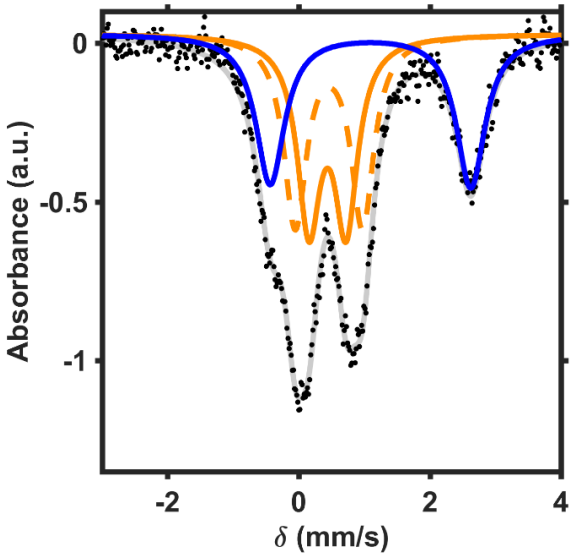

	δ (mm/s)	$\lvert\Delta E_q\rvert$ (mm/s)	Rel. %
	1.096	3.033	33
	0.434	0.547	33
	0.462	1.019	33

Figure 31. Zero applied field Mössbauer spectrum of **7-[BAr$^{F}_{4}$]** (THF solution [250 mM H_2O]; black dots) fit with three quadrupole doublets. The blue trace is assigned to high-spin Fe(II) and the orange traces are assigned to high-spin Fe(III).

Simulation details for $LFe_3O(PzNHtBu)_3Fe(OH)$ (1): The spectrum displays three discernable peaks corresponding to two quadrupole doublets in ~ 1:3 ratio. The parameters of the more intense peak are consistent with a high-spin Fe(II) assignment, while the smaller doublet could be fit a number of ways, two of which are shown here (Figure 32). Figure 32B gives parameters most consistent with an apical Fe(III). The final fit split the large doublet into three equal signals (Figure 33).

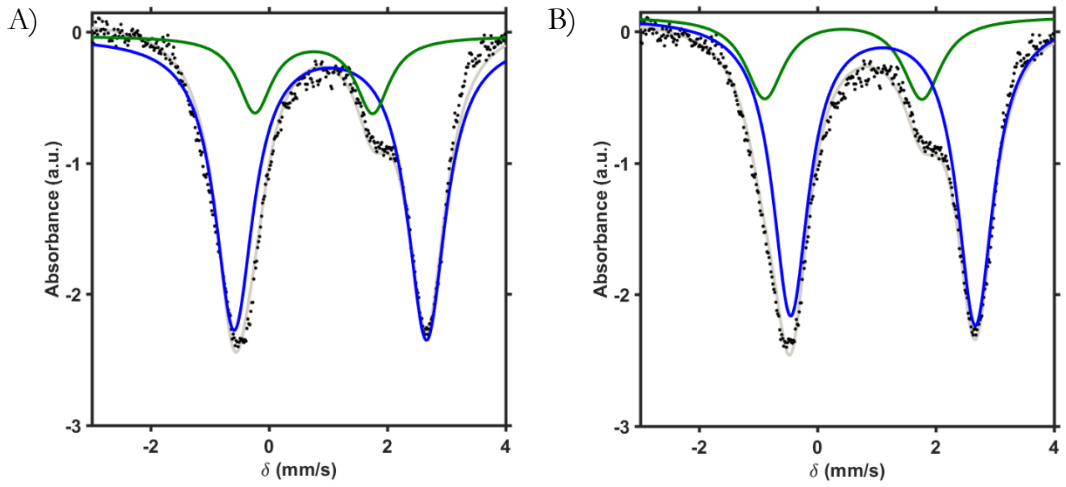

Figure 32. Mössbauer spectrum of **1** (black dots) fit with two doublets in a ~1:3 ratio (gray trace) with parameters (A) δ = 1.035 mm/s; ΔE_q = 3.255 mm/s (blue trace) and δ = 0.756 mm/s; ΔE_q = 1.993 mm/s (green trace) and (B) δ = 1.107 mm/s; ΔE_q = 3.126 mm/s (blue trace) and δ = 0.436 mm/s; ΔE_q = 2.663 mm/s (green trace).

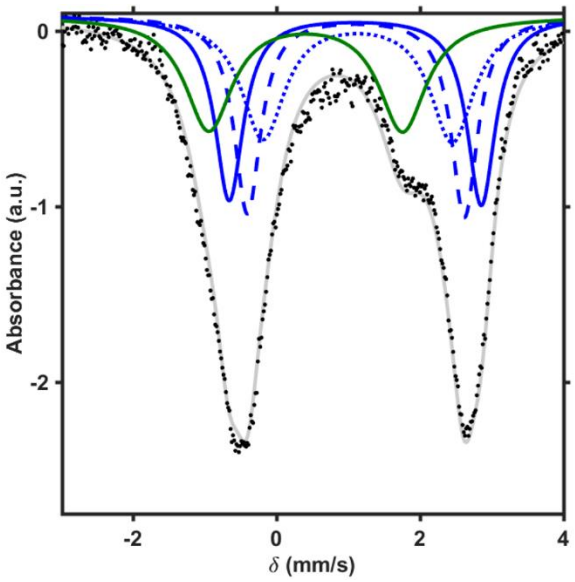

	δ (mm/s)	$\lvert\Delta E_q\rvert$ (mm/s)	Rel. %
———	1.099	3.519	25
– – –	1.109	3.029	25
– – – –	1.134	2.640	25
———	0.407	2.706	25

Figure 33. Zero applied field Mössbauer spectrum of **1** (black dots) fit with four quadrupole doublets. The blue traces are assigned to high-spin Fe(II) and the green trace is assigned as Fe(III).

Simulation details for [LFe$_3$O(PzNHtBu)$_3$Fe(OH)][OTf] (2): The spectrum displays five discernable peaks corresponding to three quadrupole doublets in ~ 1:1:2 ratio. The parameters of the most intense peak are consistent with a high-spin Fe(II) assignment, and the remainder of the signal can be fit a number of ways (Figures 34). Figure 34B gives parameters most consistent with an apical Fe(III). The final fit split the large doublet into two equal signals (Figure 35).

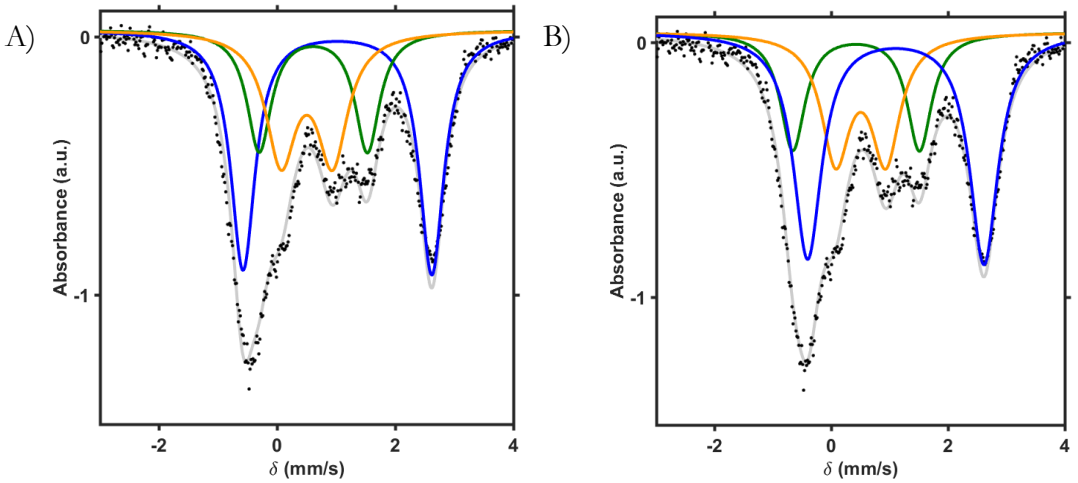

Figure 34. Mössbauer spectrum of **2** (black dots) fit with three doublets in a ~1:1:2 ratio (gray trace) with parameters (A) δ = 1.020 mm/s; ΔE_q = 3.197 mm/s (blue trace), δ = 0.502 mm/s; ΔE_q = 0.871 mm/s (orange trace) and δ = 0.612 mm/s; ΔE_q = 1.832 mm/s (green trace) and (B) δ = 1.107 mm/s; ΔE_q = 3.126 mm/s (blue trace), δ = 0.504 mm/s; ΔE_q = 0.857 mm/s (orange trace) and δ = 0.425 mm/s; ΔE_q = 2.172 mm/s (green trace).

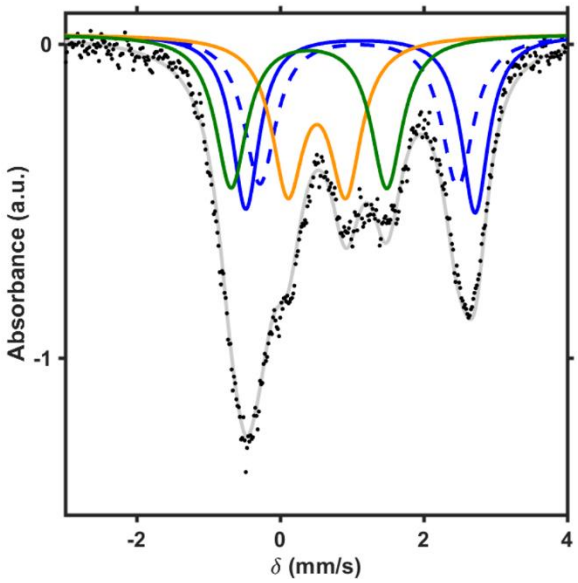

	δ (mm/s)	$\lvert\Delta E_q\rvert$ (mm/s)	Rel. %
	1.123	3.197	25
	1.100	2.757	25
	0.515	0.809	25
	0.406	2.171	25

Figure 35. Zero applied field Mössbauer spectrum of **2** (black dots) fit with four quadrupole doublets. The blue traces are assigned to high-spin Fe(II), the orange trace is assigned to high-spin Fe(III), and the green trace is assigned as Fe(III).

Simulation details for $[LFe_3O(PzNHtBu)_3Fe(OH)][OTf]_2$ (3): The spectrum displays three discernable peaks corresponding to two quadrupole doublets in ~ 1:3 ratio. The parameters of the less intense peak are consistent with a high-spin Fe(II) assignment, and the remainder of the signal can be fit a number of ways. Based on the Mossbauer parameters for the other cluster oxidation states (Figures 33 and 35), a fit was performed to obtain self-consistent parameters (i.e. making apical Fe(III) doublet with second largest quadrupole splitting). This fit led to parameters that are in good agreement for a high-spin Fe(II), two high-spin Fe(III), and the unique apical Fe(III) environment (Figure 36).

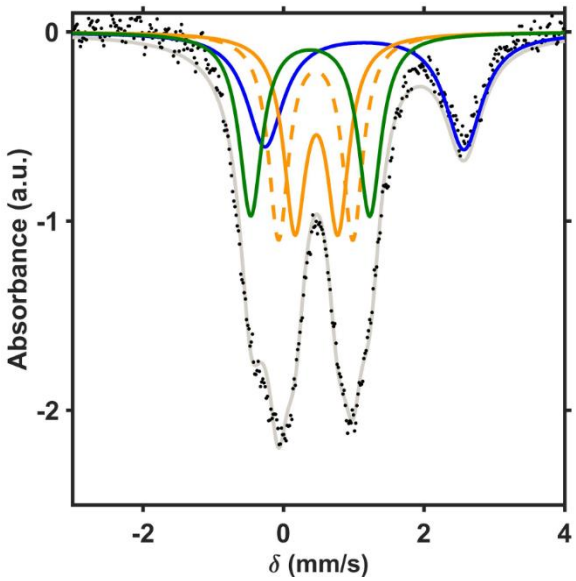

	δ (mm/s)	$\lvert\Delta E_q\rvert$ (mm/s)	Rel. %
	1.153	2.829	25
	0.469	0.613	25
	0.459	1.056	25
	0.381	1.693	25

Figure 36. Zero applied field Mössbauer spectrum of **3** (black dots) fit with four quadrupole doublets. The blue trace is assigned to high-spin Fe(II), the orange traces are assigned to high-spin Fe(III), and the green trace is assigned as Fe(III).

Simulation details for $[LFe_3O(PzNHtBu)_3Fe(OH)][OTf]_3$ (4): The spectrum displays two peaks of different intensities and shapes, consistent with multiple overlapping quadrupole doublets. In order to obtain self-consistent parameters, the spectrum was fit to four quadrupole doublets, with the doublet with the highest quadrupole splitting assigned to the apical Fe(III) (Figure 37).

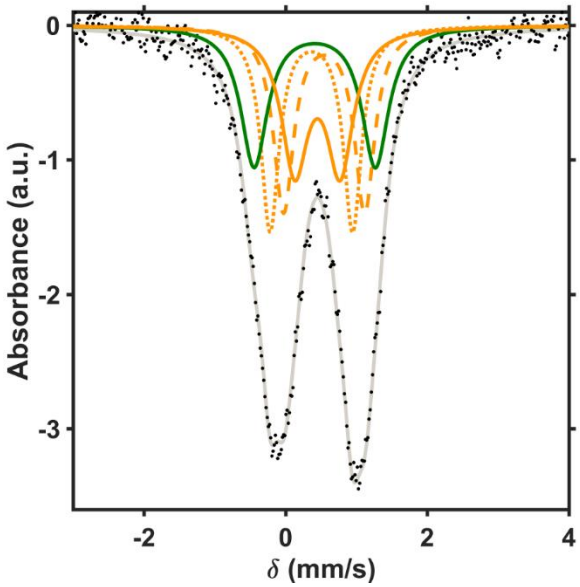

	δ (mm/s)	$\lvert\Delta E_q\rvert$ (mm/s)	Rel. %
———	0.449	0.641	25
– – –	0.543	1.145	25
– – – ·	0.363	1.166	25
———	0.411	1.712	25

Figure 37. Zero applied field Mössbauer spectrum of **4** (black dots) fit with four quadrupole doublets. The orange traces are assigned to high-spin Fe(III) and the green trace is assigned as Fe(III).

Simulation details for $LFe_3O(PzNHtBu)_3Fe(O)$ (5): The spectrum displays six discernable peaks corresponding to three quadrupole doublets in ~ 1:1:2 ratio. The parameters of the most intense peak are consistent with a high-spin Fe(II) assignment, and the remainder of the signal can be fit a number of ways (Figure 38). Figure 38C gives parameters most consistent with an apical Fe(III) and high-spin Fe(III) in the tri-iron core. The final fit split the large doublet into two equal signals (Figure 39).

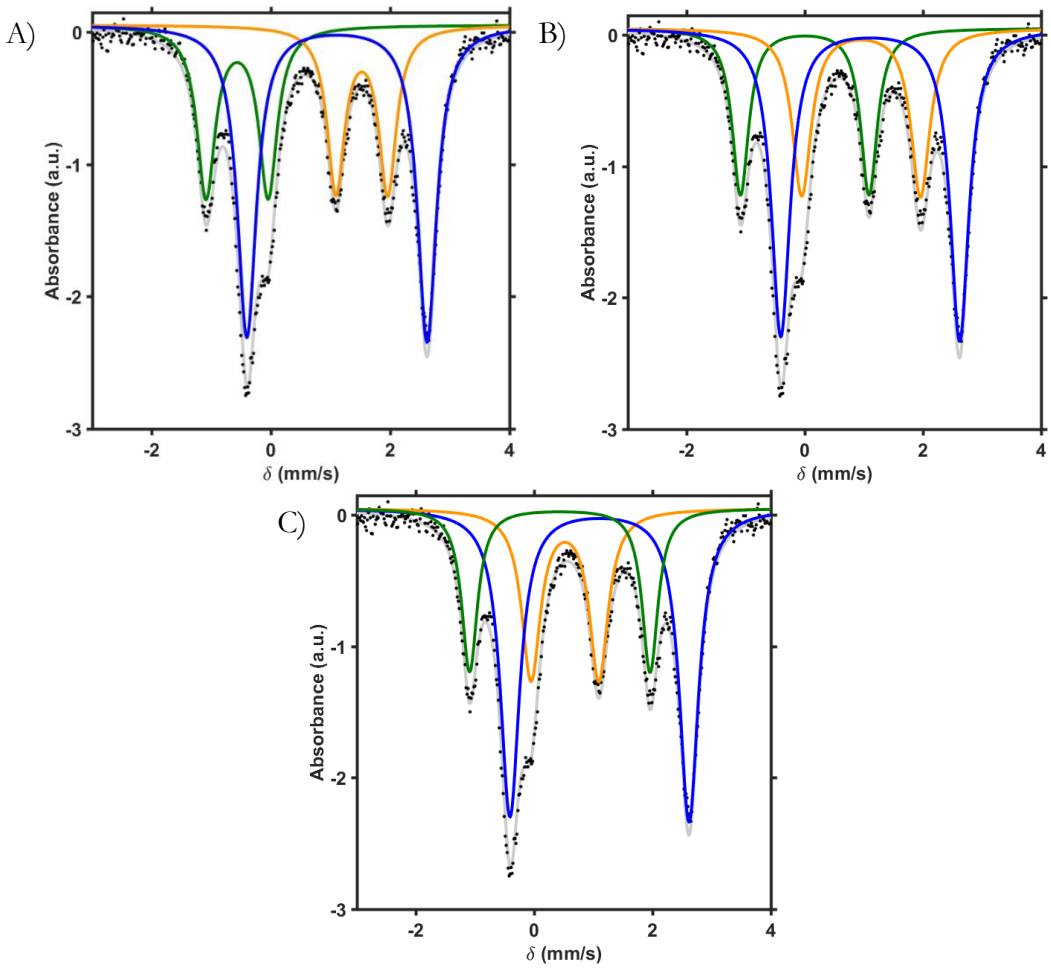

Figure 38. Mössbauer spectrum of **5** (black dots) fit with three doublets in a ~1:1:2 ratio (gray trace) with parameters (A) δ = 1.106 mm/s; ΔE_q = 3.023 mm/s (blue trace), δ = 1.522 mm/s; ΔE_q = 0.868 mm/s (orange trace) and δ = -0.569 mm/s; ΔE_q = 1.042 mm/s (green trace)., (B) δ = 1.106 mm/s; ΔE_q = 3.029 mm/s (blue trace), δ = 0.952 mm/s; ΔE_q = 2.010 mm/s (orange trace) and δ = -0.003 mm/s; ΔE_q = 2.178 mm/s (green trace), and (C) δ = 1.103 mm/s; ΔE_q = 3.027 mm/s (blue trace), δ = 0.518 mm/s; ΔE_q = 1.146 mm/s (orange trace) and δ = 0.432 mm/s; ΔE_q = 3.051 mm/s (green trace).

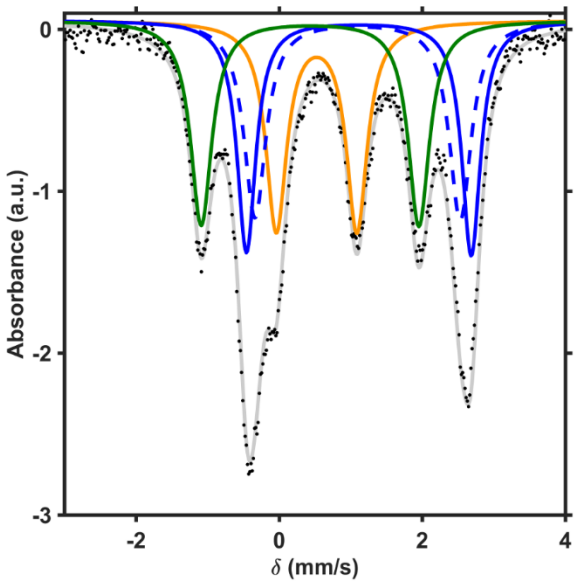

	δ (mm/s)	$\lvert\Delta E_q\rvert$ (mm/s)	Rel. %
———	1.115	3.141	25
– – –	1.097	2.869	25
———	0.524	1.126	25
———	0.433	3.042	25

Figure 39. Zero applied field Mössbauer spectrum of **5** (black dots) fit with four quadrupole doublets. The blue traces are assigned to high-spin Fe(II), the orange trace is assigned to high-spin Fe(III), and the green trace is assigned to Fe(III).

Simulation details for [LFe$_3$O(PzNHtBu)$_3$Fe(O)][OTf] (6): The spectrum displays five discernable peaks corresponding to three quadrupole doublets in ~ 1:1:2 ratio. The parameters of the most intense peak are consistent with a high-spin Fe(III) assignment, and the remainder of the signal can be fit a number of ways (Figures 40). Figure 40B gives parameters most consistent with an apical Fe(III). The final fit split the large doublet into two equal signals (Figure 41).

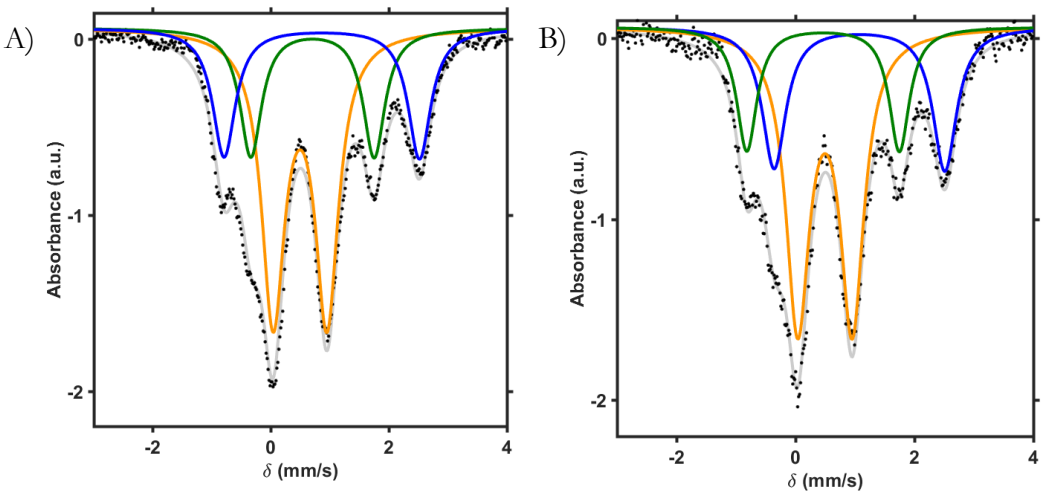

Figure 40. Mössbauer spectrum of **6** (black dots) fit with three doublets in a ~1:1:2 ratio (gray trace) with parameters (A) δ = 0.864 mm/s; ΔE_q = 3.311 mm/s (blue trace), δ = 0.495 mm/s; ΔE_q = 0.912 mm/s (orange trace) and δ = 0.706 mm/s; ΔE_q = 2.089 mm/s (green trace), and (B) δ = 1.077 mm/s; ΔE_q = 2.870 mm/s (blue trace), δ = 0.496 mm/s; ΔE_q = 0.916 mm/s (orange trace) and δ = 0.465 mm/s; ΔE_q = 2.565 mm/s (green trace).

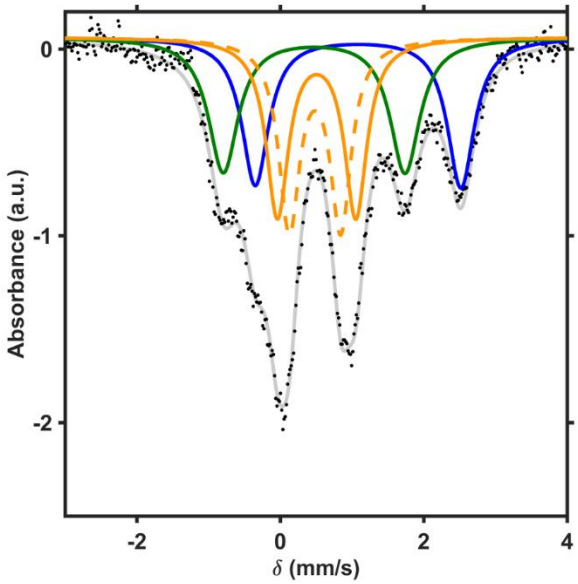

	δ (mm/s)	$\lvert\Delta E_q\rvert$ (mm/s)	Rel. %
	1.085	2.867	25
	0.507	1.093	25
	0.485	0.717	25
	0.473	2.532	25

Figure 41. Zero applied field Mössbauer spectrum of **6** (black dots) fit with four quadrupole doublets. The blue trace is assigned to high-spin Fe(II), the orange traces are assigned to high-spin Fe(III), and the green trace is assigned to Fe(III).

Simulation details for $[LFe_3O(PzNHtBu)_3Fe(O)][OTf]_2$ (7): The small peak at >2 mm/s indicated the presence of a FeII-containing impurity; NMRs of this cluster typically contained $[LFe_3O(PzNHtBu)_3Fe(OH)][OTf]_2$ (**3**) as an impurity (Figures 36 and 42). Using the parameters for **3** above, the Fe^{II} doublet was used to estimate the amount of this impurity (30 – 40% of the spectrum). This was subtracted from the data, and the remaining data appeared to be one broad doublet, similar to the $[Fe^{III}_4]$ spectrum of **4**. It was fit as four equal doublets, with the apical Fe(III) tentatively assigned to the doublet with the highest quadrupole splitting, to represent the highest value possible for this parameter (Figure 43).

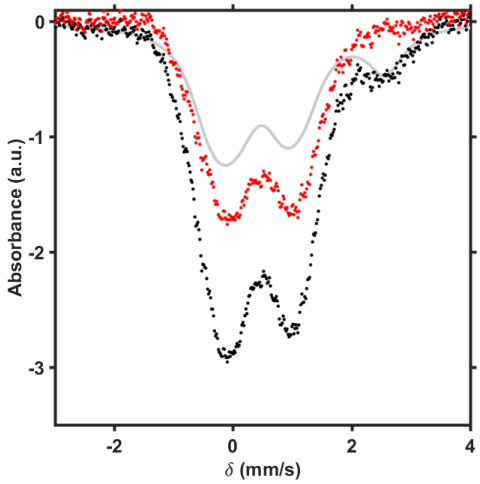

Figure 42. Mössbauer spectrum of reaction mixture containing **7** and **3** (black dots) fit with parameters to account for **3** (gray trace). The remaining signal (red dots) is assigned to the Mossbauer signal of **7**.

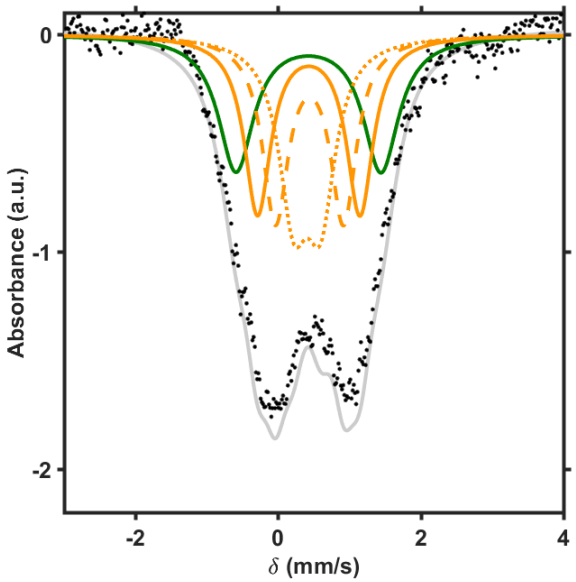

	δ (mm/s)	$\lvert\Delta E_q\rvert$ (mm/s)	Rel. %
	0.430	1.435	25
	0.440	0.953	25
	0.407	0.379	25
	0.426	2.033	25

Figure 43. Zero applied field Mössbauer spectrum of **7** (black dots) fit with four quadrupole doublets. The orange traces are assigned to high-spin Fe(III), and the green trace is assigned to the unique Fe(III).

Simulation details for $[LFe_3O(Pz)_3Fe][OTf]_2$ (2): The spectrum displays five discernable peaks corresponding to three quadrupole doublets in ~ 1:1:2 ratio. The parameters of the most intense peak are consistent with a high-spin Fe(III) assignment, and the remainder of the signal can be fit a number of ways (Figure 44). Figure 44B gives parameters most consistent with an apical Fe(II). The final fit split the large doublet into two equal signals (Figure 45).

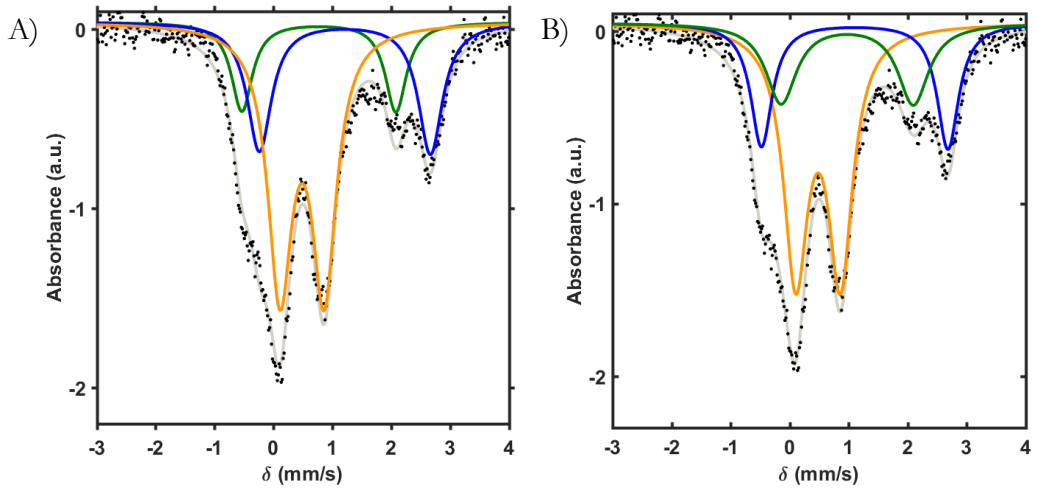

Figure 44. Mössbauer spectrum of **2** (black dots) fit with three doublets in a ~1:1:2 ratio (gray trace) with parameters (A) δ = 1.215 mm/s; ΔE_q = 2.905 mm/s (blue trace), δ = 0.487 mm/s; ΔE_q = 0.750 mm/s (orange trace) and δ = 0.773 mm/s; ΔE_q = 2.615 mm/s (green trace) and (B) δ = 1.101 mm/s; ΔE_q = 3.158 mm/s (blue trace), δ = 0.481 mm/s; ΔE_q = 0.757 mm/s (orange trace) and δ = 0.975 mm/s; ΔE_q = 2.239 mm/s (green trace).

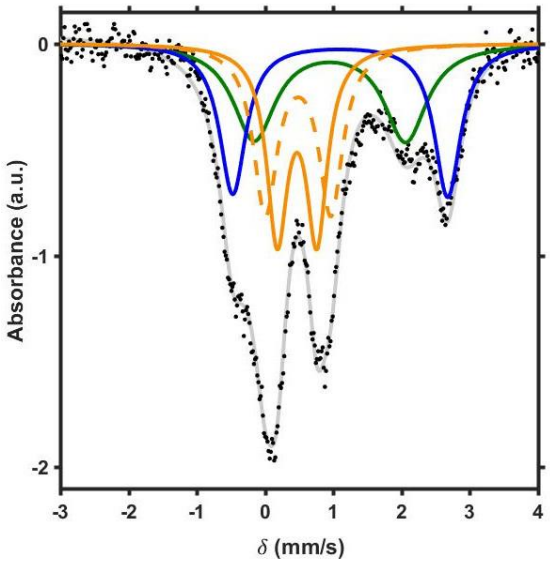

	δ (mm/s)	$\lvert\Delta E_q\rvert$ (mm/s)	Rel. %
	1.101	3.148	25
	0.469	0.580	25
	0.485	0.959	25
	0.950	2.218	25

Figure 45. Zero applied field Mössbauer spectrum of **2** (black dots) fit with four quadrupole doublets. The blue trace is assigned to high-spin Fe(II), the orange traces are assigned to high-spin Fe(III), and the green trace is assigned to Fe(II).

Simulation details for [LFe$_3$O(Pz)$_3$Fe][OTf] (3): The spectrum displays ca. four discernable peaks corresponding to three quadrupole doublets in ~ 1:1:2 ratio. The parameters of the most intense peak are consistent with a high-spin Fe(II) assignment (Figure 46A), and the remainder of the signal can be fit a number of ways (Figures 45B - D). Figure 45D gives parameters most consistent with an apical Fe(II) and high-spin Fe(III) in the tri-iron core. The final fit split the large doublet into two equal signals (Figure 46).

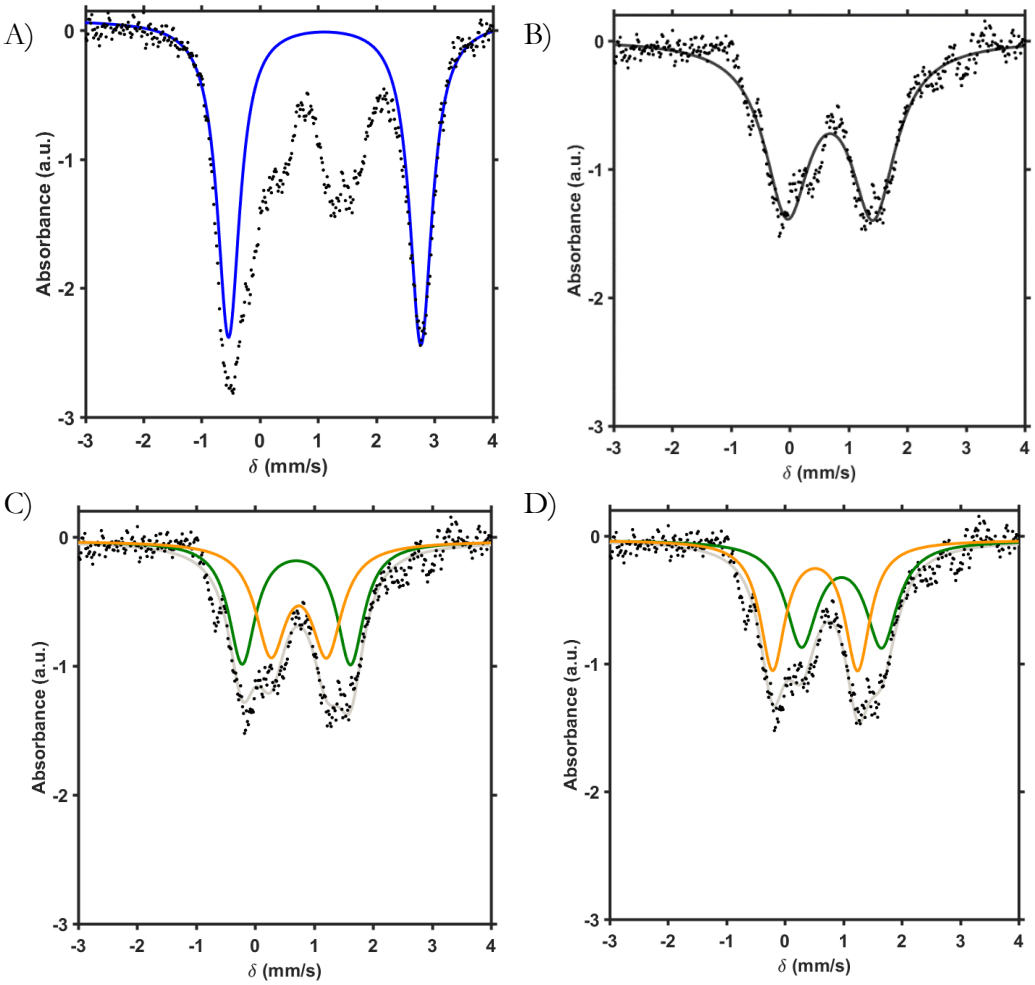

Figure 45. (A) Mössbauer spectrum of **3** (black dots) fit with a single doublet (blue trace) with parameters δ = 1.116 mm/s; ΔE_q = 3.304 mm/s, consistent with high-spin Fe^{II}. (B) Mössbauer spectrum of **3** minus the quadrupole doublet for the high-spin Fe(II) (black dots) fit with a single doublet (gray trace) with parameters δ = 0.689 mm/s; ΔE_q = 1.467 mm/s. (C) Mössbauer spectrum of **3** minus the quadrupole doublet for the high-spin Fe(II) (black dots) fit with two doublets (gray trace) with parameters δ = 0.742 mm/s; ΔE_q = 0.950 mm/s (orange trace), and δ = 0.700 mm/s; ΔE_q = 1.837 mm/s (green trace).(D) Mössbauer spectrum of **3** minus the quadrupole doublet for the high-spin Fe(II) (black dots) fit with two doublets (gray trace) with parameters δ = 0.517 mm/s; ΔE_q = 1.455 mm/s (orange trace), and δ = 0.970 mm/s; ΔE_q = 1.373 mm/s (green trace).

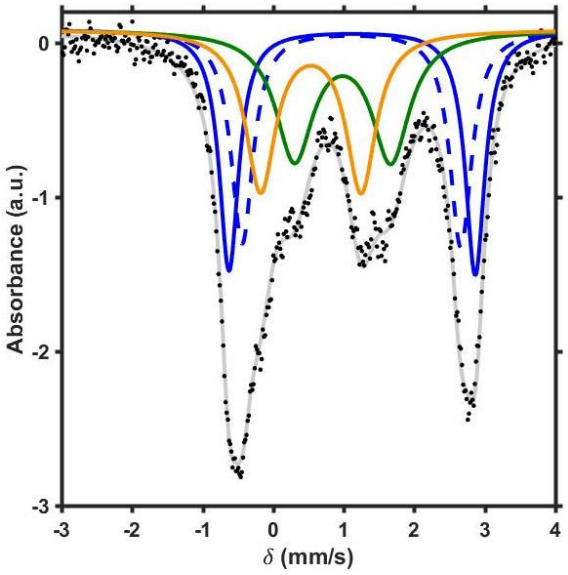

	δ (mm/s)	$\lvert\Delta E_q\rvert$ (mm/s)	Rel. %
	1.119	3.489	25
	1.110	3.099	25
	0.534	1.425	25
	0.985	1.366	25

Figure 46. Zero applied field Mössbauer spectrum of **3** (black dots) fit with four quadrupole doublets. The blue traces are assigned to high-spin Fe(II), the orange trace is assigned to high-spin Fe(III), and the green trace is assigned to Fe(II).

Simulation details for $[LFe_3O(Pz)_3Fe][OTf]_3$ (4): The spectrum displays three discernable peaks, corresponding to two quadrupole doublets in ~ 1:3 ratio. The parameters of the most intense peak are consistent with a high-spin Fe(III) assignment, and the remainder of the signal is consistent with high-spin Fe(II) (Figure 47). The final fit split the large doublet into three equal signals, one of which was assigned to the apical Fe(III) (Figure 48).

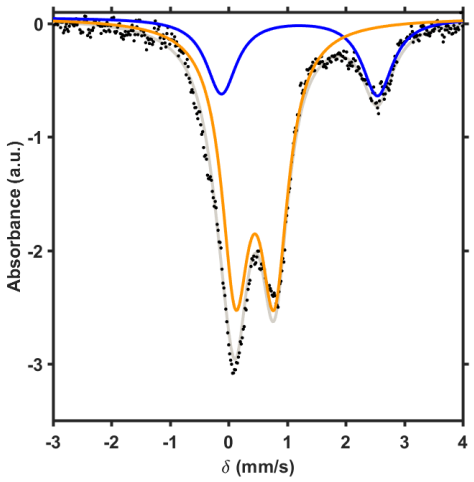

Figure 47. Mössbauer spectrum of **4** (black dots) fit with two doublets in ~ 1:3 ratio (gray trace) with parameters δ = 1.211 mm/s; ΔE_q = 2.664 mm/s (blue trace), and δ = 0.448 mm/s; ΔE_q = 0.662 mm/s (orange trace).

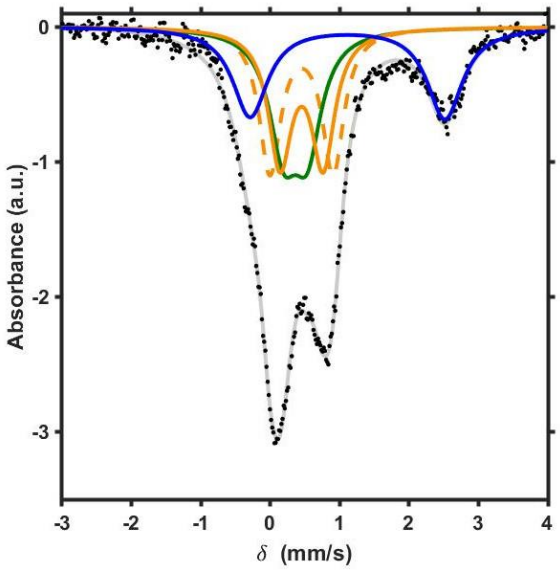

	δ (mm/s)	$\lvert\Delta E_q\rvert$ (mm/s)	Rel. %
	1.120	2.807	25
	0.458	0.621	25
	0.457	0.910	25
	0.368	0.343	25

Figure 48. Zero applied field Mössbauer spectrum of **4** (black dots) fit with four quadrupole doublets. The blue trace is assigned to high-spin Fe(II), the orange traces are assigned to high-spin Fe(III), and the green trace is assigned to the apical Fe(III).

Simulation details for [LFe$_3$O(Pz)$_3$Fe(MeCN)][OTf]$_3$ (4-MeCN): The spectrum displays three discernable peaks, corresponding to two quadrupole doublets in ~ 1:3 ratio. The parameters of the most intense peak are consistent with a high-spin Fe(III) assignment, and the remainder of the signal is consistent with five-coordinate high-spin Fe(II) (Figure 49). The final fit split the large doublet into three equal signals, one of which was assigned to the apical Fe(II) (Figure 50).

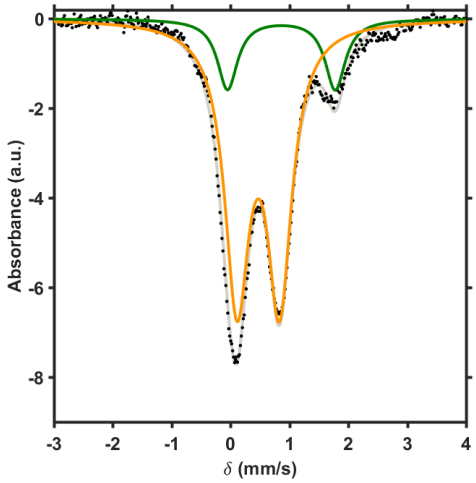

Figure 49. Mössbauer spectrum of **4-MeCN** (black dots) fit with two doublets in ~ 1:3 ratio (gray trace) with parameters δ = 0.863 mm/s; ΔE_q = 1.830 mm/s (green trace), and δ = 0.470 mm/s; ΔE_q = 0.722 mm/s (orange trace).

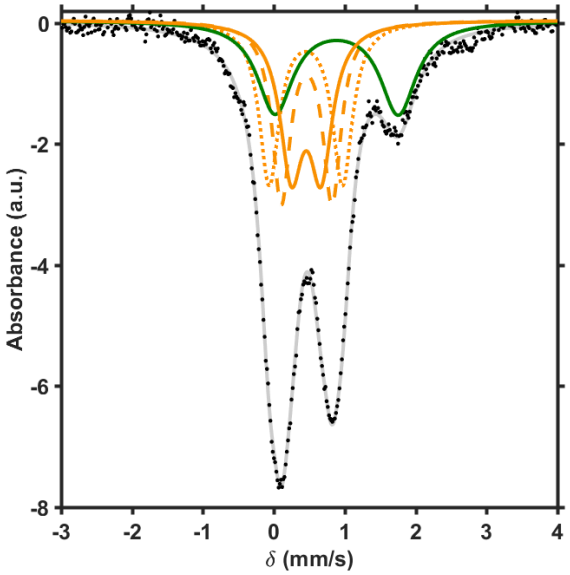

	δ (mm/s)	$\lvert\Delta E_q\rvert$ (mm/s)	Rel. %
	0.457	0.420	25
	0.464	0.716	25
	0.452	1.033	25
	0.886	1.738	25

Figure 50. Zero applied field Mössbauer spectrum of **4-MeCN** (black dots) fit with four quadrupole doublets. The orange traces are assigned to high-spin Fe(III), and the green trace is assigned to the apical Fe(II).

Simulation details for $[LFe_3O(Pz)_3Fe(OH)][OTf]_2$ (5): The spectrum displays four discernable peaks corresponding to three quadrupole doublets in ~ 1:1:2 ratio. The parameters of the most intense peak are consistent with a high-spin Fe(III) assignment, and the remainder of the signal can be fit a number of ways (Figure 51). Figure 51C gives parameters most consistent with an apical Fe(III) and high-spin Fe(II) in the tri-iron core. The final fit split the large doublet into two equal signals (Figure 52).

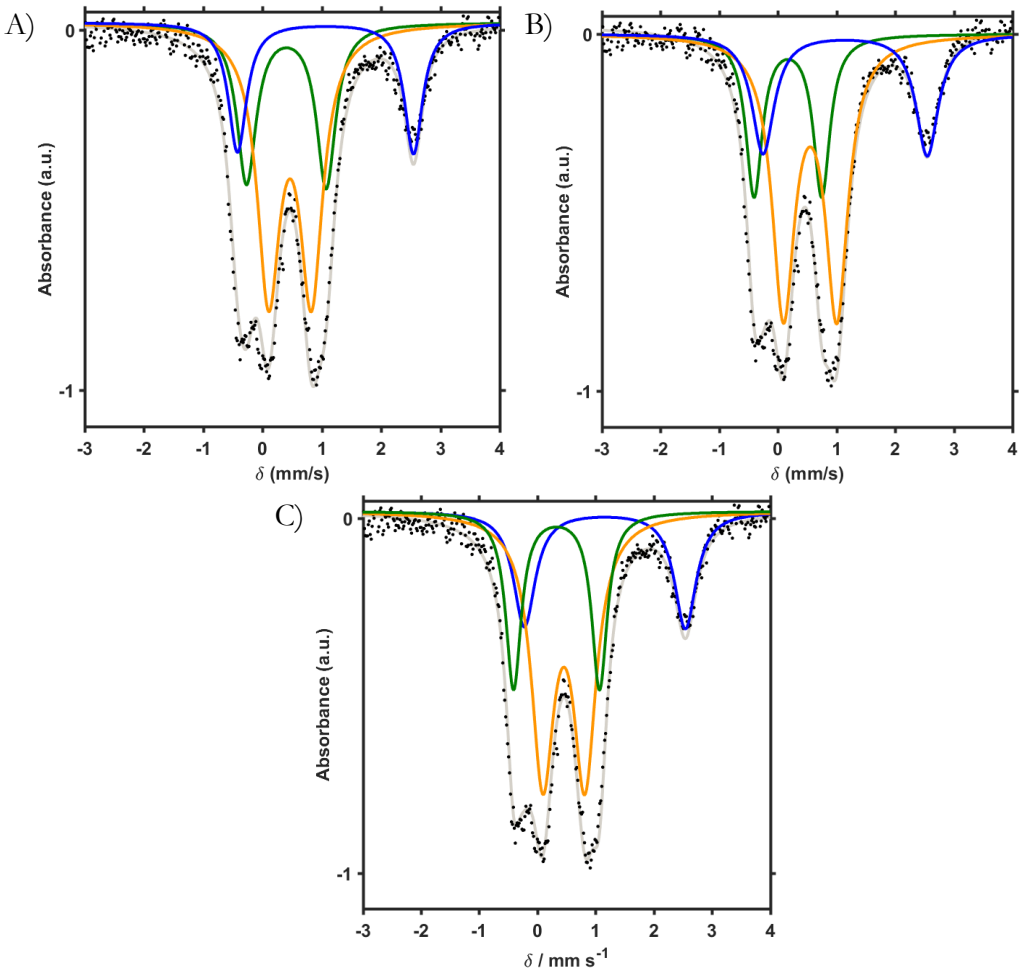

Figure 51. Mössbauer spectrum of **5** (black dots) fit with three doublets in ~ 1:1:2 ratio (gray trace) with parameters (A) δ = 0.463 mm/s; ΔE_q = 0.722 mm/s (green trace), δ = 0.401 mm/s; ΔE_q = 1.343 mm/s (orange trace), and δ = 1.062 mm/s; ΔE_q = 2.969 mm/s (blue trace), (B) δ = 0.171 mm/s; ΔE_q = 1.154 mm/s (green trace), δ = 0.549 mm/s; ΔE_q = 0.910 mm/s (orange trace), and δ = 1.147 mm/s; ΔE_q = 2.800 mm/s (blue trace), and (C) δ = 0.331 mm/s; ΔE_q = 1.478 mm/s (green trace), δ = 0.456 mm/s; ΔE_q = 0.723 mm/s (orange trace), and δ = 1.161 mm/s; ΔE_q = 2.766 mm/s (blue trace).

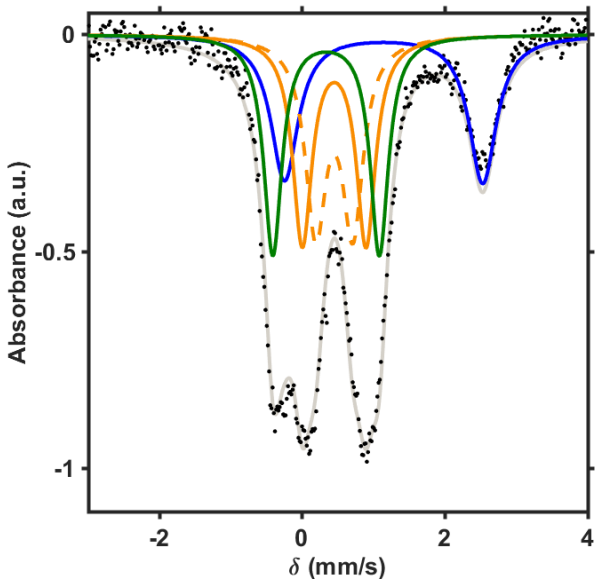

	δ (mm/s)	$\lvert\Delta E_q\rvert$ (mm/s)	Rel. %
	1.145	2.778	25
	0.452	0.893	25
	0.454	0.519	25
	0.339	1.493	25

Figure 52. Zero applied field Mössbauer spectrum of **5** (black dots) fit with four quadrupole doublets. The blue trace is assigned to high-spin Fe(II), the orange traces are assigned to high-spin Fe(III), and the green trace is assigned to the apical Fe(III).

Simulation details for $[(LFe_3O(Pz)_3Fe)_2O][OTf]_4$ (6): The spectrum displays four discernable peaks corresponding to three quadrupole doublets in ~ 1:1:2 ratio. The parameters of the most intense peak are consistent with a high-spin Fe(III) assignment, and the remainder of the signal can be fit a number of ways (Figure 53). Figure 53C gives parameters most consistent with an apical Fe(III) and high-spin Fe(II) in the tri-iron core. The final fit split the large doublet into two equal signals (Figure 54).

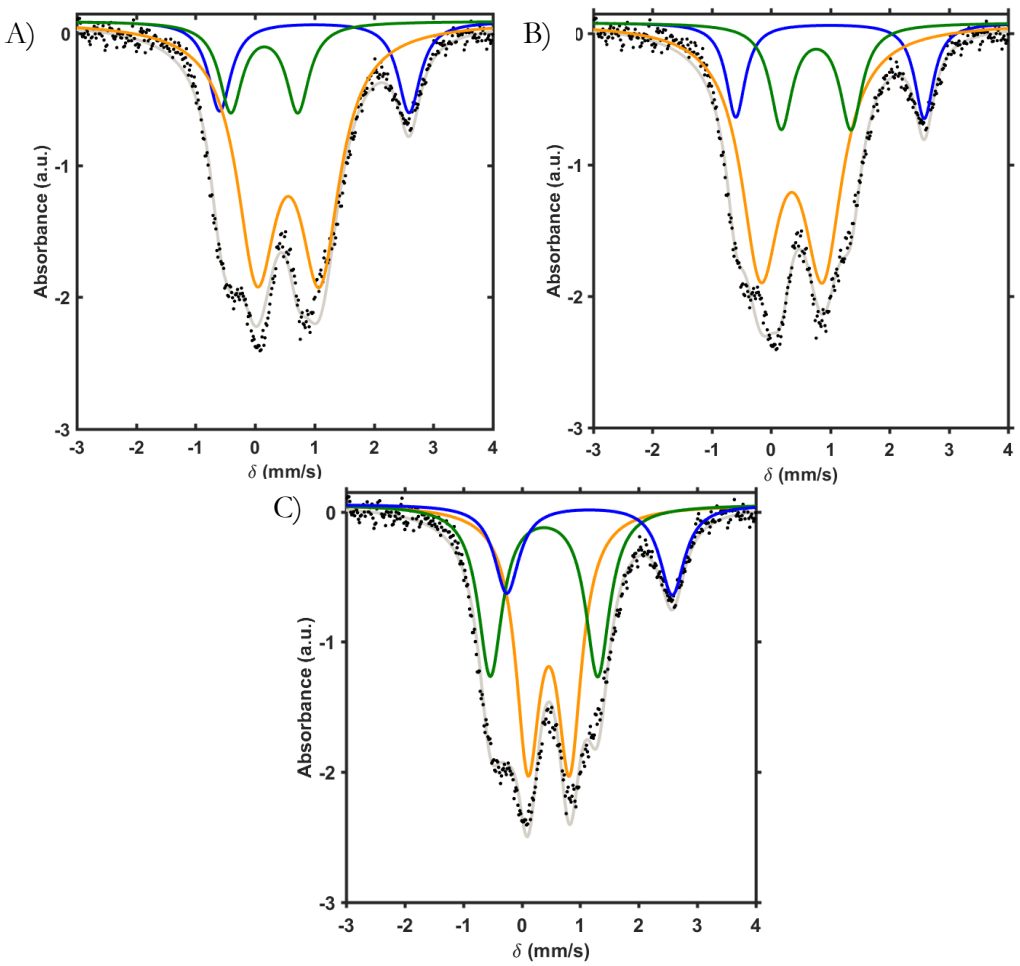

Figure 53. Mössbauer spectrum of **6** (black dots) fit with three doublets in ~ 1:1:2 ratio (gray trace) with parameters (A) δ = 0.156 mm/s; ΔE_q = 1.128 mm/s (green trace), δ = 0.560 mm/s; ΔE_q = 1.057 mm/s (orange trace), and δ = 0.999 mm/s; ΔE_q = 3.188 mm/s (blue trace), (B) δ = 0.762 mm/s; ΔE_q = 1.176 mm/s (green trace), δ = 0.350 mm/s; ΔE_q = 1.049 mm/s (orange trace), and δ = 0.995 mm/s; ΔE_q = 3.180 mm/s (blue trace), and (C) δ = 0.382 mm/s; ΔE_q = 1.835 mm/s (green trace), δ = 0.463 mm/s; ΔE_q = 0.711 mm/s (orange trace), and δ = 1.160 mm/s; ΔE_q = 2.827 mm/s (blue trace).

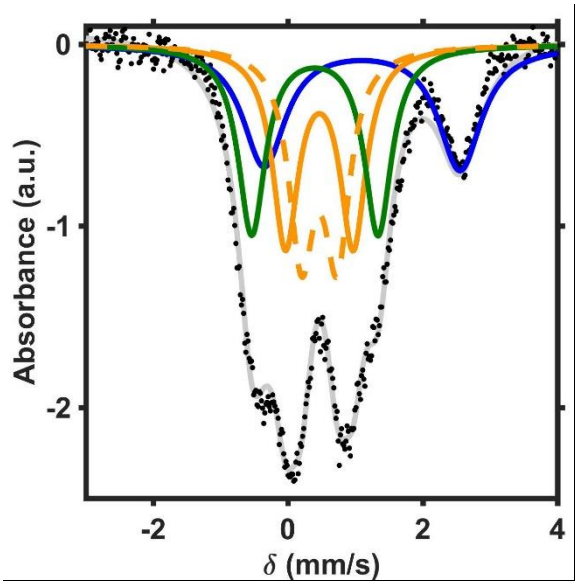

	δ (mm/s)	$\lvert\Delta E_q\rvert$ (mm/s)	Rel. %
	1.099	2.909	25
	0.645	1.005	25
	0.464	0.530	25
	0.398	1.875	25

Figure 54. Zero applied field Mössbauer spectrum of **6** (black dots) fit with four quadrupole doublets. The blue trace is assigned to high-spin Fe(II), the orange traces are assigned to high-spin Fe(III), and the green trace is assigned to the apical Fe(III).

Simulation details for putative intermediate of 2 and sPhIO: Based on variable temperature 1H NMR data, the putative intermediate is the major species at low temperature, with a small (~20%) impurity of **5**. The parameters for **5** in Figure 63 were used to model this amount of impurity, and was subtracted out (Figure 55). The remaining spectrum displays three discernable peaks corresponding to three quadrupole doublets in ~ 1:1:2 ratio. It was modeled with parameters similar to **6**, based on its similar match to the data (Figure 56).

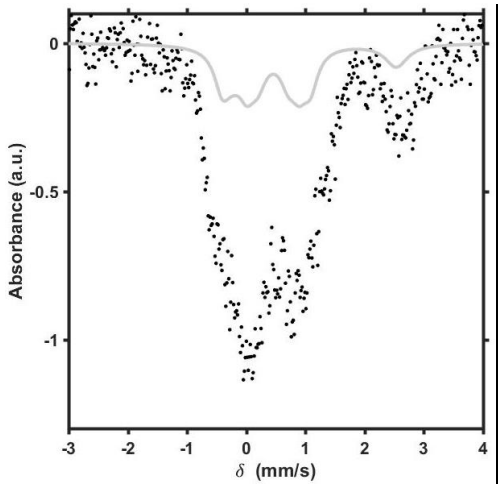

Figure 55. Mössbauer spectrum of putative intermediate between **2** and sPhIO, with ~ 20% of an impurity, **5** (black dots). The signal attributed to the impurity was subtracted from the data (gray trace).

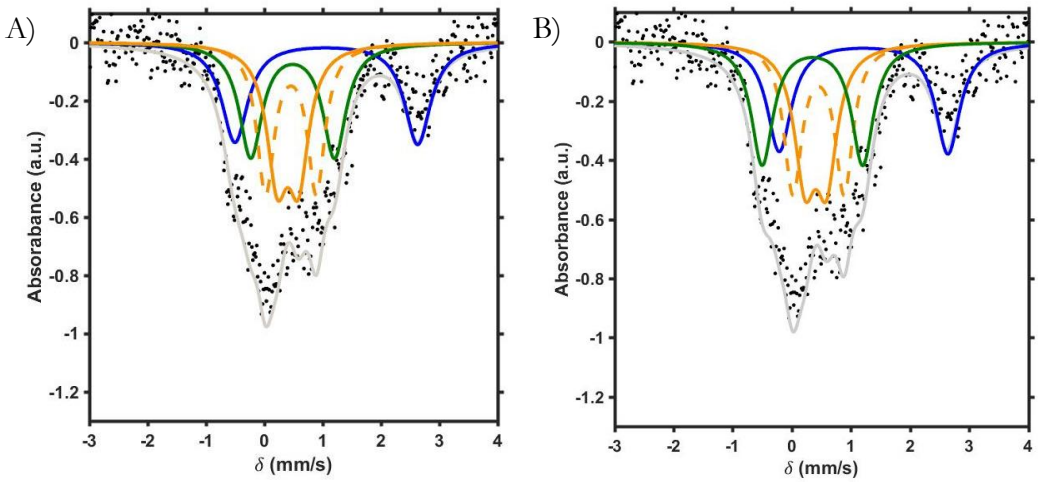

Figure 56. Mössbauer spectrum of putative intermediate between **2** and sPhIO (black dots) fit with four equally abundant quadrupole doublets (gray trace). Two potential fits with the following parameters: (A) (i) δ = 1.21 mm/s, $|\Delta E_q|$ = 2.83 mm/s (blue trace), (ii) δ = 0.41 mm/s, $|\Delta E_q|$ = 0.36 mm/s (solid orange trace), and (iii) δ = 0.45 mm/s, $|\Delta E_q|$ = 0.87 mm/s (dashed orange trace), (iv) δ = 0.35 mm/s, $|\Delta E_q|$ = 1.70 mm/s (green trace), and (B) (i) δ = 1.06 mm/s, $|\Delta E_q|$ = 3.13 mm/s (blue trace), (ii) δ = 0.40 mm/s, $|\Delta E_q|$ = 0.36 mm/s (solid orange trace), and (iii) δ = 0.46 mm/s, $|\Delta E_q|$ = 0.87 mm/s (dashed orange trace), (iv) δ = 0.49 mm/s, $|\Delta E_q|$ = 1.44 mm/s (green trace).